UNIVERSITY OF NAIROBI

Msc (environmental chemistry) thesis

SYNTHESIS AND CHARACTERIZATION OF SILVER NANOPARTICLES USING TEA EXTRACTS AND THEIR APPLICATION IN NANOBIOSENSORS

By

MOSES ONDABU OYAGI

A thesis submitted in partial fulfillment of the requirements for the award of the degree of

Masters of Science (environmental chemistry) of the University of Nairobi
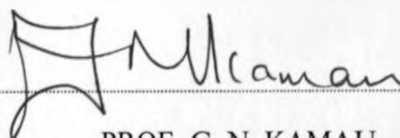
August 2012

DECLARATION

I declare that 'synthesis and characterization of silver nanoparticles using tea extracts and their application in nanobiosensors' is my own work and has not been submitted for any degree or examination in this university or any other university and that all the resources I have used or quoted have been indicated and acknowledged by means of complete references.

April 28, 2013

MOSES ONDABU OYAGI

This thesis has been submitted for examination with our approval as the university supervisors

April 26, 2013

PROF. G. N. KAMAU
DEPARTMENT OF CHEMISTRY
UNIVERSITY OF NAIROBI

April 29, 2013

DR. IMMACULATE MICHIRA
DEPARTMENT OF CHEMISTRY
UNIVERSITY OF NAIROBI

29/04/2013

DR. PETERSON M. GUTO
DEPARTMENT OF CHEMISTRY
UNIVERSITY OF NAIROBI

DEDICATION

I dedicate this work to the entire Oyagi family and to everyone who contributed to its success.

ACKNOWLEDGEMENTS

ABSTRACT

A facile reduction approach with silver nitrate, $AgNO_3$ solution and tea extracts led to polydisperse silver nanoparticles, tea-AgNPs, at room temperature. A mixture of $AgNO_3$ solution and tea extracts, extracted at $90^{\circ}C$, instantaneously turned from water colour to pale yellow and then to dark brown indicating formation of silver nanoparticles. These nanoparticles showed an absorption peak at 450 nm, along with a shoulder at 350 nm in the UV-visible spectrum corresponding to the plasmon resonance of silver nanoparticles. The absorption peak shifted to longer wavelengths (red shift) with decreasing extraction temperature. Efficiency of the tea extracts towards silver nanoparticles, AgNPs, synthesis increased with extraction temperature. These results served as a reference to determine the optimum extraction temperature. Tea extracts were acidic as evidenced by their pH values. Results of Fourier Transform Infrared Spectroscopy (FTIR) suggested involvement of same class of biomolecules in the reduction of silver ions and stabilization of the subsequent nanoparticles. Tea polyphenols, polyols, including flavonoids were identified as these biomolecules. Transmission Electron Microscopy (TEM) showed a production of spherical silver nanoparticles in the range of ca. 2-20 nm (average particle size calculated to be ca. 4.4 nm). Amount of tea extracts used affected particle size; diameters of the nanoparticles decreased with increasing amount of amount of tea extracts. X-Ray Diffraction (XRD) spectrum of the nanoparticles confirmed a formation of metallic silver. The silver nanoparticles, were highly crystalline and their diffraction peaks are indexed to (111), (200), (220) and (321) planes, corresponding to the face-centered cubic face of silver. The crystalline nature of the tea-AgNPs was further confirmed by clear lattice fringes in the high-resolution TEM image. The percent yield of AgNPs in this study was calculated to be $80 \pm 0.5\%$, suggesting the synthetic procedure to be efficient. Tea extracts in this work were very suitable for simple synthesis of AgNPs.

In their applications, tea-AgNPs enhanced current response for nanobiosensors. Drop coating tea-AgNPs onto Polyaniline (PANI) formed on platinum electrode saw a highly electroactive Pt/tea-AgNPs/ PANI nanocomposite. Characterization of PANI alone showed that this polymer can be successfully coated on platinum electrode to provide a platform for immobilization. Characterization of the tea-AgNPs nanocomposite using Scanning Electron Microscope (SEM), Ultraviolet Visible Spectroscopy (UV-vis) and Cyclic Voltammetry (CV) indicated a stable platform for the immobilization of the enzyme Cytochrome P450 (CYP2E1) to form Pt/tea-AgNPs/PANI/CYP2E1 nanobiosensors. SEM displayed large and globular morphologies for the highly active nanobioelectrodes.Tea-AgNPs/PANI nanocomposite served as a point of attachment for the enzyme as well as an efficient electron mediator between the redox centre of CYP2E1 and the electrode surface. Pt/tea-AgNPs/PANI/CYP2E1 nanobiosensors were successful in the reductive catalysis of the Ethambutol (ETH) into respective water soluble and easy excretable metabolites. The detection limits are within the nanobiosensor linear range, thereby making the nanobiosensor systems suitable for the determination of respective analytes.

Difficulties experienced in this research were mainly tied to inability to access some relevant resources online. Citations of these resources were easily accessed, but their full text articles could not be found in a database.

TABLE OF CONTENTS

List of figures

List of tables

List of schemes

List of abbreviations

AgNO$_3$	Silver Nitrate
AgNPs	Silver Nanoparticles
ATP	Adenosine Triphosphate
CCD	Charged Coupled Device
CO$_2$	Carbon Dioxide
CV	Cyclic Voltammetry
CYP2E1	Cytochrome P450, family 2, subfamily E, polypeptide 1
DNA	Deoxyribonucleic acid
DOTS	Directly Observed Treatment Short Course
DPV	Differential Pulse Voltammetry
EC	Epicatechin
ECG	(-)-Epicatechin-3- gallate
EDX	Energy Dispersive X-ray Spectrum
EGC	(-)-Epigallocatechin
EGCG	(-)-Epigallocatechin-3- gallate
EIS	Electrochemical Impedance Spectroscopy
ETH	Ethambutol
FAD	Flavoadenine
FTIR	Fourier Transform Infrared
g	Grams
GTC	Green tea Catechins
HRP	Horseradish Peroxidise

ICDD	Internationaal center diffraction Data
INH	Isoniazid
JCPDS	Joint Committee Centre Diffraction Data
mM	Millimoles
mV	Millivolts
$NaBH_4$	Sodium borohydride
NADH	Nicotinamide Adenine Dinucleotide
NADPH	Nicotinamide Adenine Dinucleotide Phosphate
NHE	Normal Nitrogen Electrode
NIR	Near Infrared
nm	Nanometres
O_2	Oxygen
PANI	Polyaniline
PANSA	Poly (8-anilino-1-naphthalene sulphonic acid)
PAS	Publicly Available Specifications
PCZ	Polycarbazole
PND	Polyindole
PPY	Polypyrrole
PRC	Polymerase Chain of Reaction
Pt	Platinum
PYR	Pyrazinamide
RIF	Rifampicin
SA	South Africa
SCE	Standard Calomel Electrode

SEM	Scanning Electron Microscope
TB	Tuberculosis
Tea-AgNPs	Tea extracts stabilized silver nanoparticles
TEM	Transmission Electron Microscopy
µl	Microliter
USEPA	United States Environmental Protection Agency
UV-vis	Ultraviolet Visible Spectroscopy
XRD	X-Ray Diffraction

CHAPTER ONE: INTRODUCTION

1.1: Why nanoparticles?

The definition of a nanoparticle, according to PAS71:2011 document developed in the UK is: "A particle having one or more dimensions of the order of 100 nm or less". Nanotechnology is a rapidly growing field of research in the world today [Sadik *et al.*, 2009]. The research explosion in this area is because nanoparticles have been found to have exceedingly better characteristics compared to their macroscale counterparts [Hu *et al.*, 2001]. To this end, nanoparticles have found great use in the worlds of technology, medicine, computers and biosensors [Bhamkar *et al.*, 2007; Zhang and Liu, 2007; Li *et al.*, 2007]. However, the method of nanoparticle fabrication has become the bone of contention. Modern conventional methods of preparing nanoparticles are expensive and involve use of environmental unfriendly reductants such as sodium borohydride [Jiang *et al.*, 2004]. Researchers are now seeking cheaper yet benign methods of preparing these nanoparticles.

Nanoparticles possess a very high surface area to volume ratio, a property that can be utilized in areas where high surface areas are critical for success. This could be for example in a catalytic industry where some nanoparticles have proven to be good catalysts. Some nanoparticles also show bactericidal effects and here a high surface area to volume ratio is also important. In biology and biochemistry nanoparticles have attracted much attention as well. This is because size of human proteins lies within the size range of nanoparticles (1-100 nm), and therefore, Scientists from the Chinese Academy of Science have even suggested using gold nanoparticles to improve Polymerase Chain of Reaction (PRC). In the production of anti-reflective optical coatings, nanoparticles have also proven valuable. Using metal oxides to coat polymeric films, anti reflective surfaces have been created.

1.2: Applications of silver nanoparticles

A possible application of silver nanoparticles is the use as a catalyst. Silver nanoparticles immobilized on silica spheres have been tested for their ability to catalyze the reduction of dyes by sodium borohydride ($NaBH_4$) [Jiang *et al.*, 2004]. Silver nanoparticles act as an electron relay, aiding in the transfer of electrons from NaB_4^- ion to the dyes, and thereby causing a reduction of the dyes. NaB_4^- ions are nucleophilic while dyes are electrophilic. It has been proven that nucleophilic ions can donate electrons to metal particles, while an electrophilic can capture electrons from metal particles. Further, it has been shown that NaB_4^- ions and dyes are simultaneously adsorbed on the surface of silver nanoparticles, when they are present together. Scanning electron microscopy (SEM) images of the particles showed that they were intact after the reaction and still immobilized on the silica spheres. This proves that the particles act as catalyst because they are not consumed in the reaction.

Silver nanoparticles have a strong tendency to agglomerate. This reduces the surface to volume ratio and thereby the catalytic effect. Therefore, a stabilizing agent is often used to prevent agglomeration. This shielding stops the growth of the silver nanoparticles, which is a disadvantage when large nanoparticles are wanted though. In this study tea extracts serves both as capping and stabilizing agents.

Another area where silver nanoparticles have been proven to be effective is in controlling and suppressing bacterial growth, for instance, Escherichia coli [Sharma *et al.*, 2009]. As a result, silver nanoparticles coated forms can be used as water filters. As the chemicals used are cheap and commonly available and the coating process is simple, it should be possible to make this available to undeveloped nations.

Optical sensors of zeptomole (10^{-21} of amole) sensitivity are other possible application using the potential of silver nanoparticles. Using the surface Plasmon effect the silver nanoparticles gain a

very high sensitivity and the measurements can be conducted in real time. The main purpose of this work was not to show that silver nanoparticles can have the stated possible applications but instead to use tea extracts in their preparation, characterize and demonstrate their effect in enhancing conductivity.

Biosensors fabricated with nanoparticles have potential applications in determining TB drugs namely; Isoniazid (INH), Rifampin (RIF), Pyrazinamide (PYR) and Ethambutol (ETH) in serum.

An electrochemical nanobiosensor consists of one part where the requisite chemical or physical processes are performed and another part for information acquisition [Muchindu *et al.*, 2010]. These nanobiosensors can be constructed if the sensing materials are modified with biological elements such as DNA and enzymes. Electrochemical nanobiosensors possess bioactive substances which are responsible for the determination of the sensitivity of the sensor and transducers which provide the sensitivity and also convert the recognition event into measurable signals [Nyholm *et al.*, 2005; Mathebe *et al.*, 2004]. By replacing classical sensor, materials with conducting polymers has achieved better selectivity and fast responses in electrochemical nanobiosensors by exploiting either the intrinsic or extrinsic functions of polymers. This has given polymers tremendous recognition in the field of artificial sensors for mimicking natural sensing organs due to their ease of coating onto electrode surfaces [Xia *et al.*, 2010; Gerard *et al.*, 2002; Adhikari *et al.*, 2004]. Immobilizing metal nanoparticles onto conducting polymers allow for even better responses and better functioning of biological compounds. The metabolism of ETH in this work is studied using the enzyme Cytocrome P450-2E1 (CYP2E1) coupled to a nanocomposite of polyaniline (PANI) and tea extracts stabilized silver nanoparticles (tea-AgNPs).

1.3: Green synthesis of nanoparticles

Green synthesis is a method for preparing a variety of materials and it involves use of environmentally benign solvents and non toxic chemicals to reduce generated hazardous wastes [Nadagouda *et al.*, 2010]. Green chemistry and chemical processes are progressively intergrating with modern developments in science and industry. Implementantion of these sustainable processes adopts the twelve fundamental principles of green chemistry [Anastas *et al.*, 2000]. These principles are geared to guide in minimizing the use of unsafe products and maximizing the efficiency of chemical processes. Scientists at the U.S. Environmental Protection Agency (USEPA) and elsewhere have emphasised the need to become environmentally conscious and conscientious. To address this issue, the main green chemistry areas need to be embraced; the choice of solvent, the reducing agent employed and capping or dispersing agent to ensure nanotechnology has a significant impact on developing green and clean technologies with considerable environmental benefits. This study sought to use bio-compatible and environmentally- benign reducing agents.

1.4: Problem statement

Today, it is possible to synthesize metallic nanoparticles with many different shapes. Nanospheres, nanorods, and nanocups are just a few shapes that have been grown. It is also possible to control the size of these particles to some extent by varying parameters such as temperature. Using analytic techniques, it is possible to determine the characteristics of nanoparticles.

Currently, most conventional methods for nanoparticles are expensive, time consuming and not environmental friendly. In the present work, economical and friendly method to prepare silver nanoparticles based on tea extracts is proposed.

1.5: Justification and novelty of the work

Globally, green chemistry and chemical processes are progressively intergrating with modern developments in science and industry. Implementantion of these sustainable processes adopts the twelve fundamental principles of green chemistry [Anastas *et al.*, 2000]. These principles are geared to guide in minimizing the use of unsafe products and maximizing the efficiency of chemical processes. This study sought to use cheap and readily available raw materials making the synthetic procedure facile and economical compared to the current conventional methods.

1.6: Objectives

The general and specific objectives of the current work were as shown below.

1.6.1: General objective

The overall objective for current research work was to study synthesis of silver nanoparticles via 'green synthesis' technology, their characterization and application in the fabrication of nanobiosensors for TB drug monitoring.

1.6.2: Specific Objectives

The specific objectives for the current research work were to:

1) Synthesize silver nanoparticles using tea extracts (tea-AgNPs).

2) Characterize tea-AgNPs using TEM, UV-Vis and XRD.

3) Apply tea-AgNPs in the reductive catalysis of Ethambutol (ETH), a common TB drug.

1.7: Rationale and motivation

This study sought to combine the bioelectronics and bioelectrochemistry of enzyme isoforms with the electron mediating ability and conductivity of AgNPs/PANI nanocomposite for the electrochemical study and modelling of TB treatment drug metabolism.

The specific application of AgNPs synthesized using tea extracts in developing the proposed nanobiosensor system for the elucidation of the metabolism of TB treatment drugs namely; Isoniazid, Rifampin, Pyrazinamide and Ethambutol is being proposed. The feasibility of this application was borne from the fact that a number of studies have suggested Cytochrome P450 2E1 (CYP2E1) to be the major enzyme catalysing tuberculosis (TB) drugs [Chen *et al.*, 2009] and AgNPs believed to enhance conductivity. The approach in this study was through the use of plant extracts to eliminate the need for chemically synthesized AgNPs in the biocatalysis of the metabolism of TB treatments drugs, by combining the use of genetically engineered CYP2E1 and cathodic polarization of the enzyme as the source of the requisite electrons. Clinically, it is important to determine the CYP2E1 profile of patients before and after the administration of Isoniazid, Rifampin, Pyrazinamide and Ethambutol in order to provide the adequate treatment and appropriate dosing of treatment. The status of the metabolism of the TB drugs in patients would be evaluated by the use of the nanobiosensor systems consisting of PANI modified with tea-AgNPs and samples of plasma and urine. This will allow on-site real time application of the nanobiosensors and point of care diagnosis for patients.

CHAPTER TWO: LITERATURE REVIEW

2.1: Synthesis of silver nanoparticles

According to Evanoff *et al.* (2004), there are extensive syntheses methods of silver nanoparticles are in use today. Some of the methods employed in the synthesis of silver nanopartcles include; molecular beam epitaxy, thermal deposition in organic solvents, laser ablation, chemical and photo-induced reduction [Sarkar *et al.*, 2009]. However, these methods are reported to use toxic chemicals, such as reducing agents and organic solvents and stabilizing agents which are not biodegradable. Nadagouda *et al.* (2008) noted that these methods pose danger to the environment and the biological systems they interact with. In addition, the controls are intricate and working conditions are nonstandard and this makes them quite expensive. As a result, there has been increasing interest in identifying environmentally friendly materials that are multifunctional. The current study employ use tea extracts. The extracts function both as reducing and capping agents for in the synthesis of silvernanoparticles. Tea extracts are highly soluble in water, have low toxicity and are biodegradable. In addition, the extracts have high levels of freely extractable phenolic compounds and are thus potential for bulk synthesis. This makes their use more cost-effective compared to conventional reagents. Green tea-catechins (GTCs) are groups of polyphenols compounds belonging to the flavonoid family. They include; (-)-epicatechin-3- gallate (ECG) (fig 2.1), epicatechin (EC) (fig 2.2), (-)-epigallocatechin-3- gallate (EGCG) (fig2.3), (-)-epigallocatechin (EGC) (2.4) and possesses various biological activities. However, until recently Nadagouda *et al.* (2008) noted that there were no reports on the preparation of noble metals using tea extracts, both which play a crucial role in many medical applications.

Anastas *et al.* (1998) noted growing concerns on the biological and environmental impact of nanomaterials prepared from conventional methods. The focus has significantly shifted to creating

nontoxic, "green" nanoparticles. This forms the basis of the current study which seeks to synthesize biocompatible and environmentally friendly silver nanoparticles. According to Sathishkumar *et al.*, (2009), silver nanoparticles have been synthesized using a wet chemistry in which tea extracts were used as reducing and capping agents. Besides use of plant extracts, use of microorganisms are widely reported in the literature. However, plant extracts has many advantages compared to the use of microorganisms [Naznin *et al.*, 2009]. For instance, scale up is easy with plant extracts as compared to microorganisms. Also, the process of maintaining cell cultures is so elaborate besides biohazards involved when using microorganisms.

Tea extracts are derived from terminal three leaves of shoots of tea plant Camellia sinensis (L.) O. Kuntze (syn. Thea sinensis L.) family Theaceae. During manufacturing, fresh green tea leaves, which are very rich in catechins, are withered, and catechin oxidation by polyphenol oxidase is prevented by steaming or by panning [Naznin *et al.*, 2009], in order to maintain the polyphenols in their monomeric forms. Black tea leaves are subjected to crushing and a full fermenting process where catechin derivatives are oxidized, resulting in the formation of the polymeric compounds thearubins and theaflavins, [Hertog *et al.*, 1993]. Depending on the application, the characteristics of the produced silver nanoparticles are manipulated by controlling parameters such as pH, temperature, concentration and the exposure time [Naznin *et al.*, 2009].

Polyphenols are also known for their powerful antioxidant property with complex structures. Other rich sources of polyphenols include: onion, apple, red wine, red grapes, grape juice, strawberries, blueberries, cranberries and certain nuts. Alcohol extracts polyphenols besides use of water.
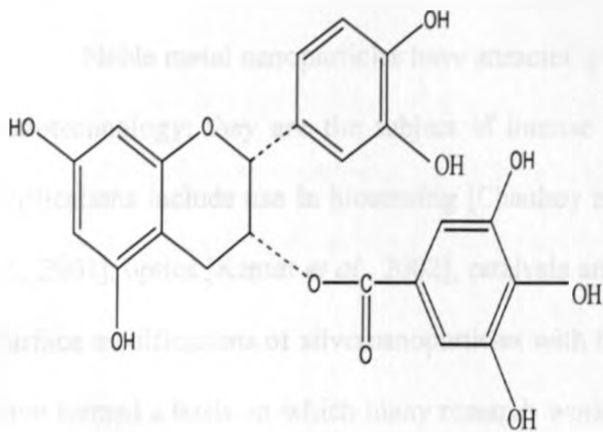
Figure 2.1 (-) Epicatechin gallate
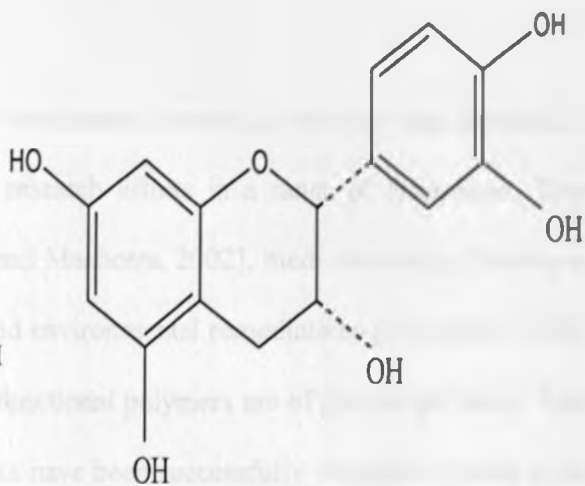
Figure 2.2 (-)Epicatechin

Figure 2.1: Structure of (-)-Epicatechin-3-gallate (ECG). **Figure 2.2:** Structure of (-)-Epicatechin (EC).
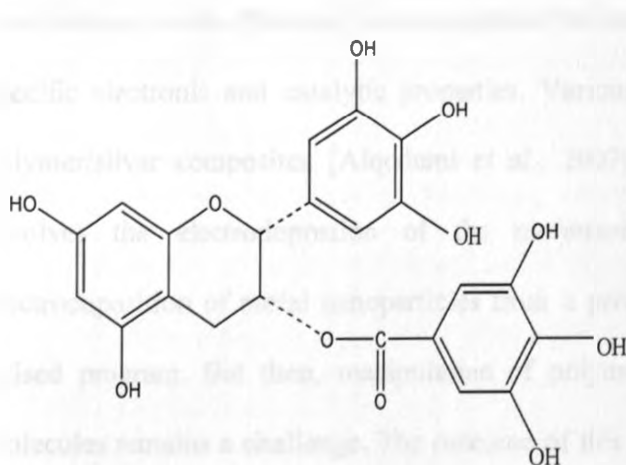
Figure 2.3 (-) Epigallocatechin gallate
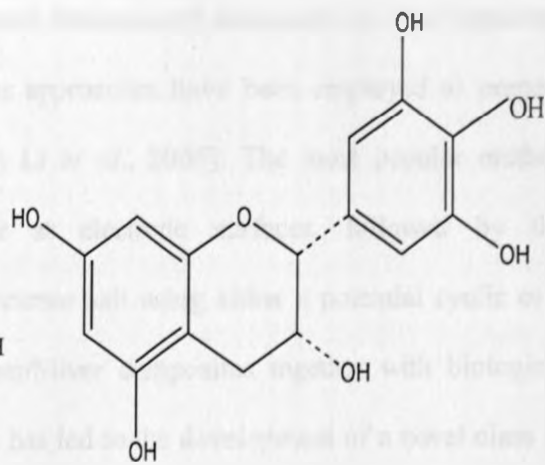
Figure 2.4 (-) Epigallocatechin

Figure 2.3: Structure of (-)-Epigallocatechin-3-gallate (EGCG). **Figure 2.4:** Structure of (-) Epigallocatechin (EGC).

2.2: Application of silver nanoparticles

Noble metal nanoparticles have attracted a tremendous interest due to their huge potential in nanotechnology; they are the subject of intense research efforts in a range of disciplines. Their applications include use in biosensing [Chaubey and Manhotra, 2002], media recording [Murray *et al.*, 2001], optics [Kamat *et al.*, 2002], catalysis and environmental remediations [Hutchison, 2008]. Surface modifications of silvernanoparticles with functional polymers are of great importance. They have formed a basis on which many research works have been successfully developed [Sadik *et al.*, 2009; Ahuja *et al.*, 2009]. Furthermore, embedding of silver nanoparticles inside the core of conducting polymers such as polyaniline and polypyrrole has become a popular and interesting aspect of polymer/metal nanocomposites synthesis as a result of the possibilities of the development of materials for chemical sensors, micoelectronic devices and electrocatalysts. This is due to the highly conductive nature of these polymers coupled with their ease of preparation and good stable environment which effectively accommodates the small dimensioned nanoparticles, thus improving specific electronic and catalytic properties. Various approaches have been employed to prepare polymer/silver composites [Alqudami *et al.*, 2007; Li *et al.*, 2005]. The most popular method involves the electrodepostion of the monomer at electrode surfaces, followed by the electrodeposition of metal nanoparticles from a precursor salt using either a potential cyclic or a pulsed program. But then, manipulation of polymer/Silver composites together with biological molecules remains a challenge. The outcome of this has led to the development of a novel class of modified electrodes in which both the charge transfer and the preservation of biological activity is obtained through experimental techniques designed to manipulate metal nanoparticles and polymers, enzymes and other biological molecules. For instance, the incorporation of sensing components in suitable matrices and the monitoring of the interaction of these components with analytes and control of enzyme, which is dependent on the interface between the enzyme and

polymers/metal composite. Such control has led to immobilization techniques suitable for anchoring the enzyme in close proximity to the electrode surface, thus preserving the biological activity. Therefore, in electrochemical devices where preservation of biological activity at the polymer/metal-enzyme interface is priority towards efficient electrode design, the charge transfer between the enzyme and the electrode is usually fast and reversible [Liu *et al.*, 2009; Mu *et al.*, 2009; Cresphilho *et al.*, 2009; Wang *et al.*, 2006].

2.3: Polymers

Traditional Polymers exhibit optical and electrical properties previously found only in inorganic systems. Consequently, they have taken charge as conductors and are widely used in a range of novel applications. Experts in various fields are combining their expertise to study organic solids that exhibit remarkable conducting properties. Organic compounds which effectively transport charge are divided into three groups; organometallic species, charge transfer complexes or ion radical salts and conjugated organic polymers. Another class of intrinsically conducting polymers or electro active conjugated polymers emerged recently. A significant requirement for a polymer to become intrinsically electrically conductive is that there should be an overlap of molecular orbitals to allow the formation of delocalized molecular wave function. Also, these molecular orbitals should be partially filled so that there is a free movement of electrons throughout the lattice [Gerard *et al.*, 2002].

2.3.1: Conducting Polymers

Conducting polymers contain π-electron backbones exerting charge mobility along the backbone contributing to their unusual electronic properties such as low energy optical transitions, electrical conductivity and high electron affinity [Gerard *et al.*, 2002]. The chemical bonding in

conducting polymers is such that one unpaired electron is produced per carbon atom in the backbone of the polymer. The carbon atoms are π bonded in a $sp^2 p_z$ configuration where the orbital of successive carbon atoms overlap providing delocalization of the electrons along the backbone of the polymer. But then, the π bonds are highly susceptible to chemical, electrochemical oxidation or reduction processes. The Increasing electrode modifications as a result of these polymers has provided new and interesting properties, which have now contributed to the wide application of conducting polymers including in electrocatalysis, rechargeable batteries, membrane separation, optoelectronic, chromatography; solar cells [Ahuja et al., 2007; Malholtra et al., 2006] and the most recent application in electrochemical biosensors. This is due to their mechanical flexibility, chemical specificities, tunable conductivities, high surface areas and easy processing [Zhu et al., 2006].

2.3.2: Synthesis of conducting polymers

There are various available methods for the synthesis of conducting polymers reported in literature. The most widely used techniques are the oxidative coupling of the monomer. This technique involves the formation of a cation radical followed by another coupling to produce a di-cation and the repetition leads to the formation of a polymer [Malholtra et al., 2006]. With the advantage of simplicity and reproducibility, electrochemical synthesis has rapidly become the preferred method of synthesizing conducting polymers [Trivedi et al., 1996].

Electropolymerization is normally carried out in a single cell compartment where a three-electrode configuration is employed, subjected to an electrochemical solution consisting of a monomer and a supporting electrolyte all dissolved in an appropriate solvent which in most cases is an acid. The polymerization can be carried out either potentiostatically where the potential is kept constant with a variation of the current with time, or galvanostatically by keeping the current

constant thereby monitoring the electrode potential. A three-electrode system employed during the polymerization comprises of a working electrode, a counter electrode and a reference electrode. Metals such gold, platinum, carbon, nickel, titanium, palladium and most recently microelectrodes are used as working electrode and function as support systems for the polymer films. Counter electrodes on the other hand, supply the current required by the working electrode. A few commonly used counter electrodes include metallic foils of nickel, platinum and gold. Reference electrodes such as SCE, NHE, silver and mercurous sulfate establish stable potentials in electrochemical reactions and are used immersed in aqueous media [Ahuja *et al.*, 2007].

Electrochemical polymerization enables the reactions to be carried out at room temperature by varying either the potential or the current with time, and the thickness of the film can be controlled. Electrochemical techniques employed in the polymerization of conducting polymers on the electrode surface are pulse, galvanostatic, potentiostatic or potential sweep techniques.

2.3.3: Types of Conducting Polymers

Conductivity of a polymer is influenced by a number of factors including polaron length, the conjugation length, and the overall chain length and by the charge transfer to adjacent molecules [Gerard *et al.*, 2002; Ahuja *et al.*, 2007; Malholtra *et al.*, 2006; Trivedi *et al.*, 1996].

2.3.3.1: Polypyrrole (PPY)

Polypyrrole is a conducting polymer which can be synthesized either chemically or electrochemically. Electrochemical sysnthesis of PPY is advantageous as the polymer produced is better conducting and the conductivity is stabilized for a long period of time [Lakard *et al.*, 2007]. Parameters such as the applied current or voltage can control the location, morphology, thickness and chemical composition of PPY. On the other hand, chemical synthesis involves the use of

particular dopants during the synthesis. These dopants include heparin and heparin sulphate and their use is based on the fact that they have an ability to increase the conductivity of the polymer to a level of 10^3 S cm^{-1}. PPY polymerisation mainly occurs on platinum electrodes where a wide variety of enzymes are immobilized where the mechanism takes place at potentials above + 600 mV. There are a number of factors affecting the film including the crystallographic structure of the underlying electrode, the nature of the electrolyte, the speed of the potential of deposition of the polymer known as the scan rate, the concentration of the monomer, the presence of anions and polyanions or in some instances surfactants and finally the pH of the solution.
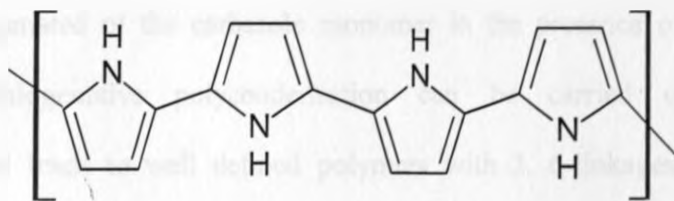
Figure 2.5: Structure of Polypyrrole.

2.3.3.2: Polyindole (PND)

Polyindole is synthesized by anionic oxidation of indole in various electrolytes. Electrochemical oxidation of indole in $LiClO_4$ containing acetonitrile produces an electrochromic polymer film with good air stability [Pandey *et al.*, 1998]. PND is green in colour in its doped state and possesses an electrical conductivity in the range of 10^{-2} to 10^{-1} S cm^{-1} depending on the nature of counter anion. The polymer is closely structured to polypyrrole and polyaniline however its conductivity is much lower although it has a better thermal stability than them. Derivatives of indole are found abundantly in natural plants and possess various physiological properties which are potential bioactive components.
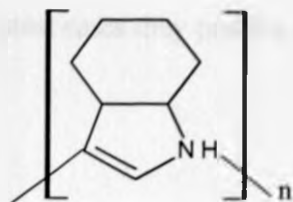
Figure 2.6: Structure of Polyindole.

2.3.3.3: Polycarbozole (PCZ)

Polycarbozole are synthesized by two main procedures. The first route is the most commonly used and involves the electrochemical or chemical oxidation of carbazole derivatives in solution [Fernandes *et al.*, 1999]. The second method employs the activation of the carbon-halogen bond of 3, 6-dihalogenated of the carbazole monomer in the presence of a zero valent nickel complex. The dehalogenative polycondensation can be carried either chemically or electrochemically and leads to well defined polymers with 3, 6-linkages. The electrochemical stability of this polymer has been observed to be less when compared to those of other conducting polymers however, this property can be enhanced by decreasing the poly disparity of the material [Tran-Van *et al.*, 2002].
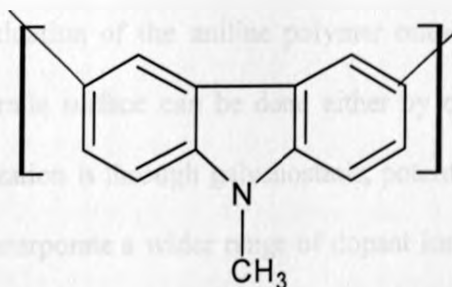
Figure 2.7: Structure of Polycarbozole.

2.3.3.4: Poly (8-anilino-1-naphthalene sulphonic acid) (PANSA)

PANSA belongs to a family of substituted naphthalenes which are normally used as fluorescent probes in the study of biologically active molecule structures. These compounds are

moderately soluble in water but in most cases they prefer a more hydrophobic environment [Catena *et al.*, 1989].
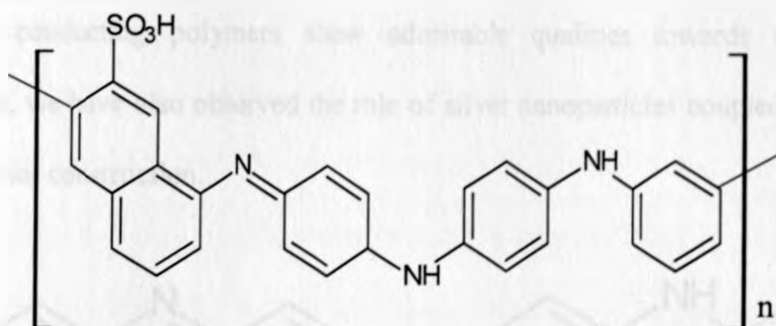
Figure 2.8: Structure of Poly (8-anilino-1-napthalene sulphonic acid).

2.3.3.5: Polyaniline (PANI)

In the present study, aniline was polymerized in the presence of hydrochloric acid to produce polyaniline (PANI) attached to platinum electrodes and incorporated the enzyme cytochrome P450-2E1 (CYP2E1) for the detection of TB treatment drugs. PANI is a conducting polymer of the semi-flexible rod polymer family that is electrically synthesized in the presence of an acidic medium by anionic oxidation of the aniline polymer onto an electrode surface. This attachment of PANI on the electrode surface can be done either by chemical or electrochemical means. Electrochemical polymerization is through galvanostatic, potentiostatic or potentiodynamic means, offering the potential to incorporate a wider range of dopant ions, since the reaction can be carried out in the presence of an appropriate electrolyte rather than a chemical oxidant. This procedure allows for film property control such as morphology and thickness allowing this polymer to be the most commonly used in biosensor preparation. For the polymer to retain its conductive property in the presence of non-acid media, it should be electrically neutral in the oxidized form of the polymer [Grennan *et al.*, 2006; Naudin *et al.*, 1998].

In biosensor development in this study, polyaniline serves as a point of attachment of the enzyme cytochrome P450-2E1 (CYP2E1), as well as a means of electron transport between the platinum electrode and the active site of the enzyme [Grennan *et al.*, 2006; Lindfors *et al.*, 2002]. Even though conducting polymers show admirable qualities towards the construction of nanobiosensors, we have also observed the role of silver nanoparticles coupled with PANI towards the nanobiosensor construction.
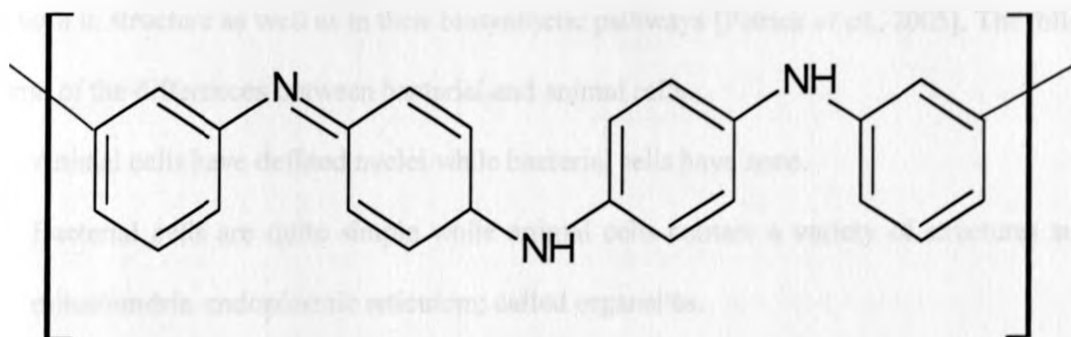
Figure 2.9: Structure of polyaniline.

2.4: Tuberculosis

Tuberculosis is a common and infectious disease caused by mycobacterium, mainly Mycobacterium tuberculosis [Wang *et al.*, 2009]. TB is spread as exhaled drops in coughs, spits or sneezes from infected individuals, [Schweon *et al.*, 2009]. This disease is a slow-growing pathogen which has the unusual propensity to shut down its metabolism during adverse conditions such as, starvation or immune stress [Wang and Chen, 2009; Hernandez *et al.*, 2008].

Treatment for TB uses antibiotics to kill the bacteria. These drugs are administered as part of the directly observed treatment short course (DOTS) therapy which is a multiple drug regimen given over a long duration of time. This regime employs an initial phase which is usually 2 months, with at least three drugs (Isoniazid (INH), Rifampin (RIF), and Pyrazinamide (PZA)) to reduce the

bacterial load as rapidly as possible. This is followed by a continuation phase employing only two drugs (INH and RIF) given for 4 months [Eoh *et al.*, 2009].

2.4.1: The bacterial cell

The antibacterial drugs, owes much to the fact that they can act selectively against bacterial cells as opposed to animal cells. This is attributed to the fact that bacterial cells and animal cells differ both in structure as well as in their biosynthetic pathways [Patrick *et al.*, 2005]. The following are some of the differences between bacterial and animal cells.

✓ Animal cells have defined nuclei while bacterial cells have none.

✓ Bacterial cells are quite simple while animal cells contain a variety of structures such as mitochondria, endoplasmic reticulum; called organelles.

✓ The biochemistry between these two cells is also very different. For instance bacterial cells are required to synthesize essential vitamins which animal cells are able to acquire intact from food. Bacterial cells therefore should have enzymes to catalyse these reactions but animal cells should not since the reactions are not required.

✓ The bacterial cell has a cell membrane and a cell wall while an animal cell only has a cell membrane. The cell wall is crucial to the survival of bacterial cells as they have to survive a wide range of environments and osmotic pressures, whereas animal cells do not (Patrick *et al.* 2005).

The DOTS regime has contributed significantly towards the falling incidences of TB. However, incomplete implementation of the campaign has been a major cause of the high occurrences of the drug resistant strains of Mycobacterium tuberculosis coupled with the spread of HIV/Aids in tuberculosis-endemic regions [Wallis *et al.*, 2009; Zvavamwe *et al.*, 2009]. Patients

with fully susceptible TB develop secondary resistance during the TB therapy as a result of inappropriate dosing of treatment. Table 2.1 below lists a few second-line TB drugs.

Table 2.1: List of first and second-line TB drugs [Eoh *et al.*, 2009].

Name of drug	Dosage/Adult(as necessary)
First-line	
Isoniazid	300 mg/day
Rifampicin	600 mg/day
Pyrazinamide	25 mg/kg/day
Ethambutol	15-25 mg/kg/day
Steptomycin	15 mg/kg/day
Second-line	
Amikacin	15 mg/kg/day
Aminosalicylic acid	8-12 g/day
Capreomycin	15 mg/kg/day
Ciprofloxacin	1500 mg/day, (divided)
Clofazimine	200 mg/day
Cycloserine	500-1000 mg/day, (divided)
Ethionamide	500-750 mg/day
Ofloxacin	600-800 mg/day
Rifabutin	300 mg/day

In the present study, the nanobiosensor developed was used to detect Ethambutol (ETH), one of the first line TB drugs.

2.4.2: Ethambutol (ETH)

This is a synthetic, water-soluble, heat-stable compound, the dextro isomer of the structure shown below (Figure 2.10), is dispensed as the dihydrochloric salt [Bennet *et al.*, 2007; Meyers *et al.*, 1980; Craig *et al.*, 1990]. Commercially, ethambutol is referred to as Myambutol.
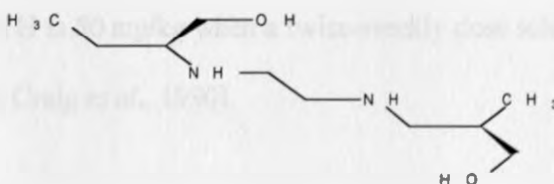
Figure 2.10: Structure of Ethambutol.

2.4.3: Mechanism of Action, Resistance and Pharmacokinetics of Ethambutol

Susceptible strains of mycobacterium tuberculosis and other mycobacteria are inhibited in vitro by ETH with concentration 1 - 5 µg/mL. ETH functions by inhibiting the synthesis of arabinogalactan, an essential component of the mycobacterial cell wall. It enhances the activity of lipophilic drugs such as RIF that cross the cell wall primarily in lipid domain of this structure.

ETH is well absorbed the gut following ingestion of 25 mg/kg. A blood level peak of 2 – 5 µg/mL is reached in 2 – 4 hours with about 20 % of the drug excreted in faeces and 50 % in urine in unchanged form. In cases of renal failure, ETH accumulates and therefore drug dose should be reduced in half if creatine clearance is less than 10 mL/min. ETH is able to cross the blood-brain barrier only if the meninges are inflamed. Cerebrospinal fluid is highly variable, ranging from 4 – 64 % of serum levels in the setting of meningeal inflammation. Similarly to all antituberculous

drugs, resistance to ETH emerges at a very rapid rate when the drug is administered alone. Therefore, ETH is always administered in combination with other antituberculous drugs. As of date, there is no known documentation about the mechanism of resistance [Bennet *et al.*, 2007; Meyers *et al.*, 1980; Craig *et al.*, 1990; Clayton *et al.*, 2001].

2.4.4: Clinical uses of Ethambutol

ETH hydrochloride, 15 – 25 mg/kg, is usually given as a single daily dose in combination with rifampicin and INH. Higher doses are however required for the treatment of tuberculosis meningitis. The dose of ETH is 50 mg/kg when a twice-weekly dose schedule is used [Bennet *et al.*, 2007; Meyers *et al.*, 1980; Craig *et al.*, 1990].

2.5: Biosensors

It is an analytical device which incorporates intimate and deliberate combination of a specific biological compound and a physical entity. The role of the biological compound is to create a recognition event while the physical entity transduces the recognition event [Paddle *et al.*, 1996]. Interest in the development and exploitation of analytical devices for quantification, detection and monitoring of specific chemical species and reactions has led to the emergence of biosensors. With biosensors representing an emerging new trend in diagnostic technology, metabolites such as urea, cholesterol, glucose and lactate in whole blood have been estimated [Gerard *et al.*, 2002].

A successful biosensor possesses some beneficial features such as; the bioactive substance should be highly specific for the purpose of the analyses. The reaction, which takes place, should be independent of physical parameters such as stirring, pH and temperature as this would allow minimal pre-treatment of samples prior to analysis. The obtained response after analysis should be accurate, precise, reproducible and linear over the useful analytical range and should be free from

electrical noise. Most importantly, the complete biosensor should be cheap, small, portable and capable of being operated by semi-skilled operators [Ryne-Byrne *et al.*, 1997].

Bioactive materials are compounds or materials that give biosensors their selectivity characteristics. In most cases these biocomponents undergo reactions with their respective analytes which is denoted by an end signal. Within a biosensor the recognition biocomponent incorporated possess some level of sensitivity although it may be vulnerable to extreme conditions such as pH, ionic strength and temperature. Most of these biocomponents including antibodies, enzymes and cells have very short lifetimes in solution and have to be fixed in a suitable matrix. Therefore, immobilization of these compounds is of critical importance to allow their stability although their activities are sometimes reduced [Gerard *et al.*, 2002].

2.5.1: Enzymes

An enzyme is a protein with a three dimensional structure which acts as a catalyst in chemical reactions. Research has shown that most enzymes have been successfully used in the construction of biosensor. These components are unique since they are a combination of selectivity and sensitivity and they allow for a wide selection of transducers to be used [Conn *et al.*, 1987]. An enzyme sensor can be considered as a combination of transducer and a thin enzymatic layer, which is responsible for measuring the concentration of the substrate. In close proximity to the enzyme, is the sensitive surface of the transducer with the assumption that there is no mass transfer across the interface. The external surface of the biocomponent is kept immersed in solution containing the substrate of interest. In doing so, the substrate migrates towards the interior of the enzyme and is converted into products when it reacts with the immobilized enzyme [Adhikari *et al.*, 2004]. Signals of enzyme sensors are strongly influenced towards their application by inhibition, temperature and pH dependence [D'Orazio *et al.*, 2003] which in turn affects the reaction between the immobilized

enzyme and the substrate. In this study cytochrome P450-2E1 was employed in the construction of a nanobiosensor used for detecting ETH.

The stability of the immobilized enzyme with respect to time, temperature, storage conditions and at times experimental variables are critical performance indicators that should be noted [Worsfold *et al.*, 1995]. The most popular and highly recommended is the storage of enzyme under normal operating conditions in an appropriate buffer solution. During the procedure, special attention should be placed to aspects such as pH, temperature, ionic strength and the incorporation of impurities as they have an effect on the enzyme during immobilization [Worsfold *et al.*, 1995].

2.5.2: Transducers

The role of transducers in biosensor construction is to convert a biochemical signal to an electronic signal. Transducers allow biosensors to be more specific and more selective. Depending on the nature of the biocomponents interaction with the analyte of interest, suitable transducing systems can be adapted in the biosensor construction [Conn *et al.*, 1987].

2.5.3: Cytochrome P450 Enzymes

The study uses Cytochrome P450-2E1 (CYP2E1, EC 1.14.14.1), towards the construction of a biosensor responsible for the catalytic biotransformation of ETH using tea-AgNPs.

2.5.3.1: occurrence of Cytochrome P450 Enzymes

Cytochrome P450 enzymes also known as Iron Porphyrin enzymes were first investigated by Warburg and at that time they were referred to as cell pigments. He discovered that in the dark carbon monoxide had an inhibitory factor on respiration cells, however upon illumination, respiration was resumed. Knowing this fact, Warburg then suggested that in respiration a

compound of iron was involved. Upon a close examination of the photo effect, it was discovered that a specific wavelength was involved with a characteristic absorption wavelength of iron hemachromogen containing porphyrins. Warburg then came to the conclusion that the respiratory pigments were similar to these compounds [Key et al., 1966]. It was Keilen who revisited the work MacMunn continued from Warburg who discovered that at specific wavelengths a pigment was absorbed in several cells hence giving them the name cytochrome. Thereafter, all examined cells containing this pigment, could be readily observed on reduction due to a change in light absorption [Key et al., 1966].

2.5.3.2: Kinetic reactions of Cytochrome P450 Enzymes

Cytochrome P450 enzymes belong to a multigene family of heme enzymes which catalyse the NADPH – dependant monoxygenase and reactions of different exobiotic and endobiotic liphophilic substrates. The unique ability of these enzymes is based on the fact that they can hydroxylate non-activated carbon atoms (C-H bonds). Metabolism of substrates produces products which serve as regulators in cells or are excreted from organisms. These enzymes are capable of metabolizing over 1,000,000 chemicals and involve about 60 distinct classes of biotrasformation reactions; N-, O-, or S-, demethylation, dealkylation, S- oxidation, epoxidation, aliphatic oxidation, reductive dehalogenation and sulfoxide formation [Shumyanteva et al., 2005; Bistolas et al., 2005]. They are also involved in mono-oxygenation reactions which are very useful as they are responsible for the hydroxylation of a number of compounds including steroids, fatty acids, drugs, food additives, fungi, bacteria, [Harris et al., 2001] alkanes and polyaromatic and polychlorinated hydrocarbons.

In man most of the C ytochrome P450 enzymes are found in the liver with a remarkable amount also found in the small intestine, around the microsomal part of the cytoplasm, in the

endoplasmic reticulum as well as in the mitochondria. Enzymes isolated from the mitochondria are known as steroidogenic cytochrome enzymes since they are situated in single cell organisms and are phylogenetically older. Usually they consist of an iron-sulphur protein, NADPH and NADH-dependant reductase (on FAD-type flaovoprotein) and Cytochrome P450 enzyme. Steroidogenic enzymes are responsible for steroid synthesis as well as other substances which are required for maintaining the cell wall integrity. Another form of these enzymes evolved from steriodogenic enzymes over one billion years ago are known as xenobiotic enzymes. Xenobiotic enzymes are located in the smooth endoplasmic reticulum of cells, while some studies indicate that they have evolved during the period of plant-animal differentiation. They are constituted by NADPH: P450 reductase (FAD-and FMN- containing flavoprotein) and cytochrome P450 enzyme [Iwuoha *et al.*, 2003]. The strength of these enzymes lies in their ability to metabolise foreign biological substances.

2.5.3.3: Kinetics of catalytic reaction

Cytochrome P450 enzymes consist of iron-protoporphyrin IX active sites with axial thiolate of cysteine residues as fifth ligands. Resting cytochrome P450 enzymes are in the ferric form (Fe^{3+}), one electron reduction of a ferric form leads to a ferrous state (Fe^{2+}). In most cases, these enzymes are octahedral and because of unpaired electrons in their 3d orbitals, they are practically all paramagnetic. Due to the presence of protoporphyrin IX, heme enzymes exhibit characteristic visible absorption spectra however, their spectra differ according to the identities of the lower axial ligands donated by the protein and the oxidation state of the iron, while the identities of the upper axial ligands are donated by the substrates. The source of electrons in this type of system is from flavoproteins, ferrodoxin like proteins, NADPH [Harris *et al.*, 2001], the mediator or an electrode.

The mechanism for substrate hydroxylation by cytochrome enzymes, involves the following steps although there are still several details that still remain unsolved.

Step 1: When the substrate binds to the hexa-coordinated low-spin ferric enzyme (has few unpaired electrons), water is excluded from the active site and changing the state of heme iron to a high spin (with more unpaired electrons) substrate-bound complex. The high spin ferric enzyme (Fe^{3+}) has a more positive reduction potential and thus is much easier reduced. This causes a decrease in polarity which is accompanied by a positive shift [Bistolas *et al.*, 2005] or lowering of the redox potential by 110 mV to 130 mV which makes the first electron transfer step thermodynamically favourable, from its redox partner NADH or NADPH [Shumyanteva *et al.*, 2005].

$$Fe^{3+}\text{-RH}$$
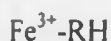
Step 2: The transfer of the first of two electrons from one of the redox partners reduces the ferric iron to the ferrous enzyme (Fe^{2+}) and this process is called reduction.

$$Fe^{2+}\text{-RH}$$
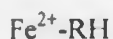
Step 3: This form of the enzyme can now bind molecular oxygen resulting in a ferrous-dioxygen ($RH\text{-}Fe^{2+}\text{-}O_2$) complex. This process is usually faster than the previous one since, since in the cell there is much more oxygen than the substrate.

Step 4: A second electron transfer takes place along with a proton gain forming an iron-hydroperoxo (Fe^{3+} - OOH) intermediate [Bistolas *et al.*, 2005].

Step 5: The O_2^{2-} reacts with two protons from the surrounding solvent, breaking the O-O bond to release a water molecule and a highly reactive iron-oxoferryl intermediate. One hydrogen atom is abstracted from the substrate by the intermediate to produce a one electron reduced ferry species (Fe^{IV}- OH) and a substrate radical. On the other hand, the ferryl species reacts with the C – H bond of the substrate in a concerted reaction without the radical intermediate formation.

Step 6: The final step of the process is the formation of the enzyme product complex and the release of the product. The low-spin state of the enzyme is then regenerated [Bistolas *et al.*, 2005]. The reaction mechanism of these enzymes is illustrated in the following scheme:
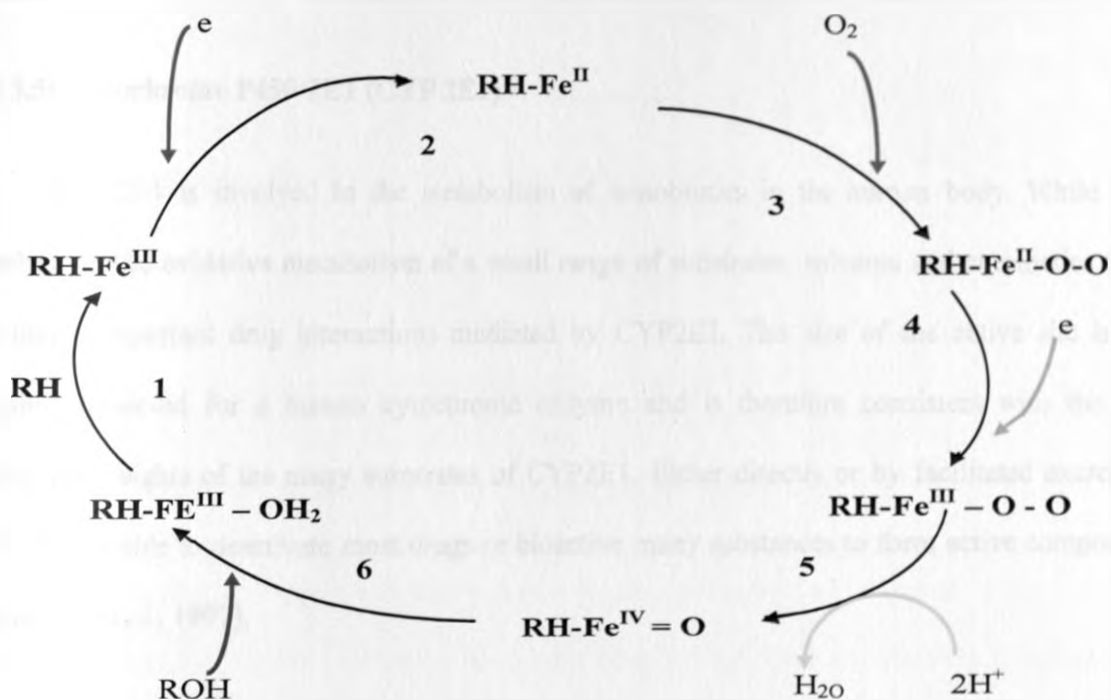
Scheme 2.1: Mechanism pathway of CYP enzymes.

2.5.3.4: Classification of Cytochrome P450 Enzymes

The classification system of enzymes was developed based on certain similarities amongst different enzymes such as amino acid sequence homology. This system is based on the principle that the more similar the structure of the enzymes, the more closely are they both phylogenetically and functionally. Cytochrome P450 enzymes are grouped into families represented by the first number; example in cytochrome P450-2E1 (CYP2E1) the first number represented is 2. The idea behind this grouping is based on the fact that all the enzymes in the same family have at least 40%

amino acid sequence homology. Furthermore, these families are further grouped into subfamilies where at least 55% of the amino acid sequences are homologous among the enzymes. The subfamilies are denoted by an alphabetical letter which in cytochrome P450-2E1 (CYP2E1) is E. The last number which is 1 represents the gene that codes for the enzyme [Ghosal *et al.*, 2005].

2.5.3.5: Cytochrome P450-2E1 (CYP 2E1)

CYP2E1 is involved in the metabolism of xenobiotics in the human body. While it is involved in the oxidative metabolism of a small range of substrates, solvents and anesthetics there are many important drug interactions mediated by CYP2E1. The size of the active site is the smallest observed for a human cytochrome enzyme and is therefore consistent with the low molecular weights of the many substrates of CYP2E1. Either directly or by facilitated excretion, CYP 2E1 is able to deactivate most drugs or bioactive many substances to form active compounds [Spracklin *et al.*, 1997].

Among the available cytochrome P450 enzymes, CYP2E1 is notable for resulting in toxicity greatly affecting the liver. This is due to the fact that CYP2E1 comprises over 50 % of the hepatic cytochrome P450 mRNA and 7 % of the hepatic cytochrome P450 protein. On the other hand, CYP2E1 is expressed at lower levels in a variety of extra-hepatic tissues where it is thought to play a role in the metabolism of certain endogenous molecules. Levels of CYP2E1 together with resulting toxicity vary respectively in response to diabetes, alcohol consumption, fasting and obesity. Therefore, the action and behavior of CYP2E1 can have either a positive or negative influence on human health and drug metabolism [Porubsky *et al.*, 2008; de Groot *et al.*, 2002]. The structure of CYP 2E1 is illustrated in Figure 2.11 (Porubsky *et al.* 2008).
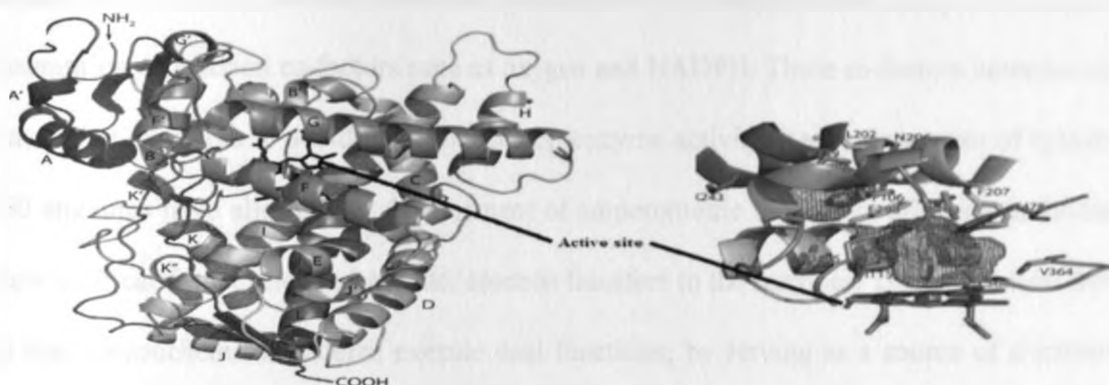
Figure 2.11: Distal face of CYP2E1 rainbow colored from N terminus (blue) to C terminus (red) also showing the active site of CYP2E1[Porubsky *et al.*, 2008].

2.5.3.6: Application of Cytochrome P450 Enzymes in biosensors

Cytochrome P450 enzymes play a key role in detoxication of bioactive compounds and hydrophobic xenobiotics coming from both outside (drugs, medicines, environment pollutants and food supplements) and those formed inside cells (steriods, prostaglandins, cholesterol, saturated and unsaturated fatty acids and others) in living organisms. Computer assisted processes or enzymatic experimental systems are used to predict metabolic transformations of physiological active substances and to investigate possible metabolic pathways. As a result electrochemical systems based on recombinant forms of cytochrome P450 appear to be the most popular as they enable standardization of analysis formats [Shumyantseva *et al.*, 2007]. Therefore, characterization of cytochrome P450 enzymes is a key issue in pharmacokinetics, toxicokinetics and in the regulation of some endogenous metabolic pathways.

Currently, the activity of cytochrome P450 enzymes is determined from the rates of formation of metabolites while the metabolic concentration requires development and maintenance

of methods for each metabolic pathway studied. Another possible applicable method irrespective of the substrate of interest and the individual cytochrome P450 enzyme under study is to measure the consumption of reaction co-factors such as oxygen and NADPH. These co-factors however need to be available in excess to avoid any influence on enzyme activity. Redox properties of cytochrome P450 enzymes have allowed the development of amperometric biosensors allowing individuals to follow their catalytic cycles and monitor electron transfers to the enzymes. This is resultant from the fact that electrochemical systems execute dual functions; by serving as a source of electrons and have the ability to substitute partner proteins. The success of an amperometric biosensor relies on the electrical communication between an electrode and an enzyme; however in most cases the bulk nature of the protein may impede the redox site from direct electron transfer. In addition to this, macromolecular impurities and enzyme denaturing may also impede electron transfer. On the other hand, specifically binding the enzyme to the electrode surface may overcome these problems. While various immobilization techniques have been reported to establish electrical communication in enzyme-electrode construction, methods must often be designed empirically for the specific enzyme under study [Joseph *et al.*, 2003; Shumyantseva *et al.*, 2007; Bistolas *et al.*, 2005]. The ultimate approach is the direct or mediatorless electron transfer from the redox electrode to the redox active group of the CYP enzyme.

Alternatively to this approach, cytochrome enzymes are attached to electrodes by introducing electroactive bridges; also known as mediators covalently coupled to the enzyme. Such redox relays have been bound at specifically selected sites generated by protein engineering or randomly.These approaches are relevant since cytochrome P450 and enzyme based electrodes may be used as biosensors in patient point-of-care diagnostics, the investigation of drug interferences and high-throughput screening.

This is clearly demonstrated by the study reported herein where CYP2E1 was used as a bioactive component coupled to a nanostructured silver nanoparticles-polyaniline nanocomposite. This nanobiosensor was successfully used in the determination of tuberculosis treatment drug, ETH.

2.6: Electrochemical techniques

Electrochemical techniques refer to methods in which there is an interaction between electrical power and matter [Chaubey and Malhotra, 2002]. Electrochemistry is the study of chemical and physical reactions as a result of electrons through oxidation and reduction reactions. The reactions take place in a solution at the interface of an electron conductor or electrode. Besides being cheap and efficient way of dealing with some of the most pollutants, it is also showing itself to be a greener alternative to several other forms of cleanup now available. Advantages associated with using electrochemistry include versatility, energy efficiency, safety, selectivity, environmental compatibility, cost effectiveness and amenability to automation. Although there is a tremendous interest in using electrochemistry to develop novel and healthier ways of manufacturing and using chemical products, there is a broader need to address pollution, waste and deteriorating health issues produced by non-green processes of the past. Because electrochemistry can generate charged species; whether through oxidation or reduction at will, and can deal with solid, liquid, or gaseous pollutants, it only takes a scientists imagination to develop new methods of use [Lesney *et al.*, 2002]. The term redox comes from the two concepts of reduction and oxidation. It can be explained in simple terms [Lesney *et al.*, 2002]: Oxidation describes the loss of electrons/ hydrogen or gain of oxygen or increase in oxidation state by a molecule, atom or ion. Reduction describes the gain of electrons/hydrogen or a loss of oxygen/ decrease in oxidation state by a molecule, atom or ion.

2.6.1: Sweep techniques

Potential sweep techniques such as cyclic voltammetry (CV) have been applied to an increasing range of systems over the past couple of decades. The mathematical descriptions of these techniques have been sufficiently developed to enable kinetic parameters to be determined for variety of reaction and mechanisms. This technique indicates the potentials at which processes occur while from the sweep rate dependence, the involvements of coupled homogeneous reactions are identified and complications of absorption are detected. Because of these capabilities, CV is nearly always the technique of choice when studying a system for the first time [Lesney *et al.*, 2002].

Voltammetry is a microanalysis technique analyzing only small proportions of a given solution at solid working electrodes. In Linear Sweep Voltammetry (LSV); which is the simplest of these techniques, the potential is swept from an initial potential E_1, to a final potential E_2 at a known scan rate before halting the potential. Figure 2.12 shows a linear sweep voltammogram for the reduction of a solution phase analyte illustrated as a function of scan rate [Lesney *et al.*, 2002].
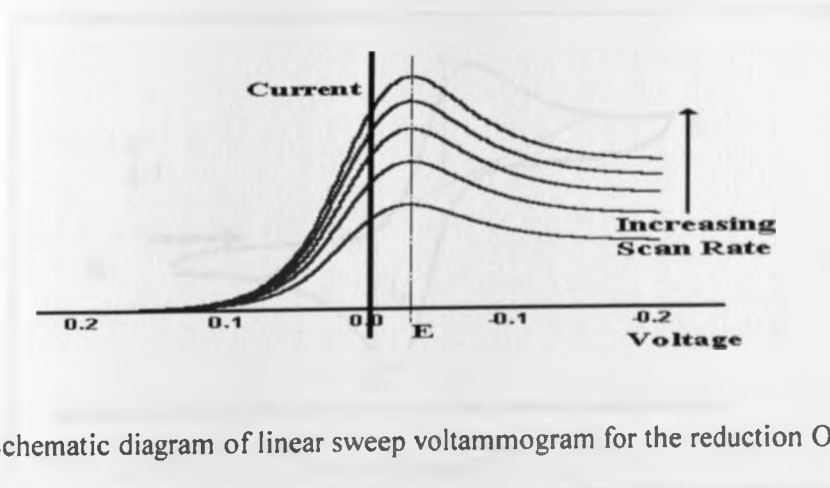
Figure 2.12: Schematic diagram of linear sweep voltammogram for the reduction $O + ne^- \rightarrow R$, at a solid electrode, shown as a function of the scan rate.

A more useful technique is CV where the potential is similarly swept from initial potential E_1, however at the end of the linear sweep, the potential scan is reversed rather than terminated. The potential sweep may be reversed again, halted or continued further to another value, E_3 In an experiment where a reverse in the potential occur, then the potential at which the reverse occurs is known as the switch potential (E_λ). The scan rate between E_1 and E_λ is the same as that between E_λ and E_1 while the values of the scan rate $v_{forward}$ and $v_{reverse}$ are always written as positive values.

When studying a system for the first time using CV, it is common to start by carrying out quantitative experiments so as to get a feel for the system before proceeding semi-quantitative and finally quantitative ones. In a study voltammograms are recorded over a wide range of sweep rates and various values of potential; as seen in Figure 2.13. Commonly there are several peaks of similar shape on either sides of the voltammogram, however if fully reversible, their magnitudes can be identified. These peaks indicate either oxidation or reduction taking place

at the forward or reverse scan. Just as other forms of voltammetry, the magnitude of the current (I) is proportional to the concentration and this parameter is usually the most commonly observed.
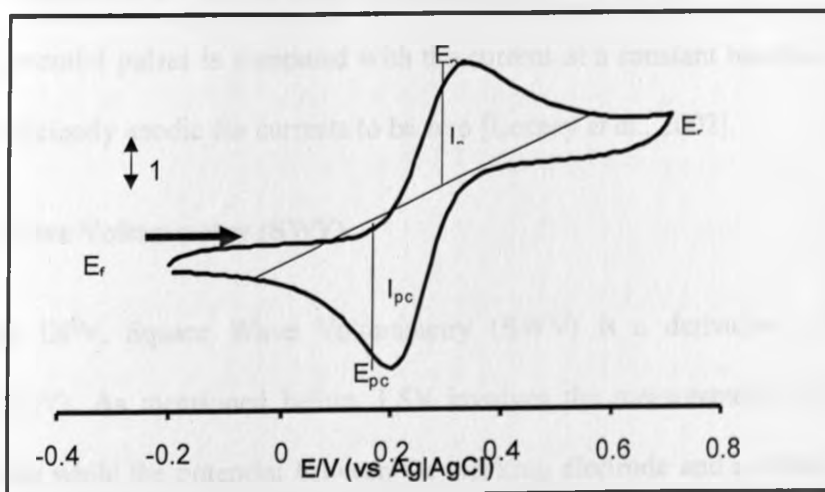
Figure 2.13: Schematic diagram of cyclic voltammogram for the reduction of an analyte at a solid electrode.

-33-

2.6.2: Pulse Voltammetry (PV)

Pulse voltammetric techniques have been developed largely to provide enhanced sensitivity in analytical application. Pulse methods were developed in the 1950s to improve the sensitivity of polarographic measurements made by pharmaceutical companies. Presently two techniques dominate the analytical field; Differential and Normal Pulse Voltammetry. Pulse techniques are based on rate decay differences of the charging and the faradaic currents following a potential step (or "pulse"). The rate of decay of the charging current is considerably faster than the decay of the faradaic current [Lesney *et al.*, 2002]. What happens is that the charging current decays exponentially, while the faradaic current (usually for a diffusion-controlled current) decays as a function of $1/(time)^{1/2}$. At a time of $5R_uC_{dl}$ after the potential step, the charging current is negligible. R_uC_{dl} is known as the time constant for the electrochemical cell, and it ranges from μs to ms. After this time, the measured current consists solely of the faradaic current; that is, measuring the current at the end of a potential pulse allows discrimination between the faradaic and charging currents [Lesney *et al.*, 2002].

On the other hand, in Normal Pulse Voltammetry (NPV) the current resulting from a series of ever larger potential pulses is compared with the current at a constant baseline potential and is chosen to be sufficiently anodic for currents to be zero [Lesney *et al.*, 2002].

2.6.3: Square Wave Voltammetry (SWV)

Just like DPV, Square Wave Voltammetry (SWV) is a derivative of Linear Sweep Voltammetry (LSV). As mentioned before, LSV involves the measurement of the current at a working electrode while the potential between the working electrode and a reference electrode is swept linearly with time. In SWV, a potential waveform is applied to the working electrode while pairs of current are measured for each wave cycle. The oxidation or reduction of involved species

is observed as peaks in these current signals at potentials where the species began to be oxidized or reduced [Chang et al., 2010; Shumyantseva et al., 2005].

2.6.4: Electrochemical Impedance Spectroscopy (EIS)

Electrochemical impedance spectroscopy (EIS) has been part of the electrochemistry community for more than a century and is one of the most effective techniques for studying the properties of substances at the electrode/electrolyte interface. In an electrochemical system the electrode/electrolyte interface is fully characterized when impedance measurements have been made in a whole range of frequencies. Unfortunately, to make such measurements takes relatively long, somewhere between about 30 min and a few hours, depending on the frequency range and the stability of the electrochemical system because the frequency needs to be scanned for the measurements. Often by the time the impedance measurements are made the electrochemical system has been changed completely in the full frequency range, particularly at a given potential. Therefore, in EIS the system under study is exposed to a sinusoidal voltage of small amplitudes (5 - 10 mV) with variable frequency (0.1 Hz - 100 kHz), and the resulting change in impedance (Z) is measured. The imaginary impedance (Z_{Im}) and the real impedance (Z_{Re}) are recorded as a function of the applied frequency with the result that the Nyquist plots (Z_{Im} vs Z_{Re}) is fitted to simple electrical equivalent circuits (EECs). By fitting EECs, important information of the interface such as solution resistance (Rs), electron transfer resistance (R_{ct}), Warburg element (R_w) and double layer capacitance (C_{dl}), are measured [Chang et al., 2010; Shumyantseva et al., 2005].

No matter how well the measurement is made, the current flowing at an electrode/electrolyte interface always contains nonfaradaic components. Electrons are transferred across the interface as illustrated in Figure 2.10 [Chang et al., 2010] with the charge transfer resulting in both faradaic and nonfaradaic components. The faradaic component arises from the electron transfer through a

reaction across the interface by overcoming an appropriate activation barrier, also known as the polarization resistance (R_p), along with (Rct) while the nonfaradaic currents results from charging the double layer capacitor (C_d) [Siddiqui *et al.*, 2010].
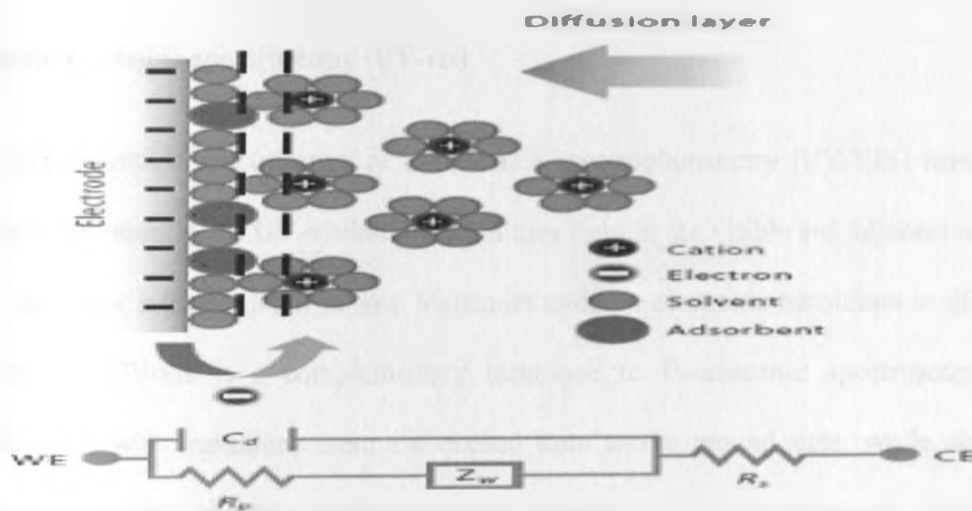
Figure 2.14: Schematic diagram of an electrified interface in which the electrode is negatively charged and where counter anions are aligned along the surface [Siddiqui *et al.*, 2010].

Typically, in electrochemical systems three types of Nyquist plots (a very useful tool for determining the stability of systems) are observed:

(1) A straight line, which illustrates a diffusion-limited process with facile electron transfer;

(2) A semicircle that is accompanied by a straight line at low frequencies of the spectrum; and

(3) A semicircle, which represents an electron transfer-limited process with its diameter (x-axis) corresponding to the Rct at the electrode [Yoo *et al.*, 2003].

For biosensor applications, a semicircle spectrum with negligible noise from an unmodified electrode is preferable as it provides higher sensitivity. This was clearly demonstrated by the work of Sun *et al.* (1998) where a single-stranded deoxyribonucleic acid was immobilized on gold electrode with self-assembled aminoethanethiol monolayer for DNA electrochemical sensor

applications. The success of the DNA electrochemical sensor was based on hybridization with a complementary DNA and the intercalation of daunomycin as a hybridization indicator to form a dsDNA: daunomycin system on the gold electrode surface. The DNA sensor was shown to be highly stable and sensitive.

2.6.5: Ultraviolet-visible spectroscopy (UV-vis)

Ultraviolet-visible spectroscopy or ultra-visible spectrophotometry (UV/VIS) involves the spectroscopy of photons in the UV-visible region. It uses light in the visible and adjacent near ultra violet (UV) and near infrared (NIR) ranges. Molecules undergo electronic transitions in this region of the spectrum. UV-vis is a complementary technique to fluorescence spectroscopy, since fluorescence deals with transitions from the excited state to the ground state, while absorption measures transitions from the ground state to the excited state. UV/Vis spectroscopy is applied in analytical chemistry for the quantitative determination of different analytes, such as highly conjugated organic compounds, transition metal ions and biological macromolecules with analyses usually carried out in solutions [Skoog *et al.*, 1992].

The solutions of transition metal ions may be coloured so as to absorb visible light because d electrons within the metal atoms can be excited from one electronic state to another. The presence of other species such as ligands or certain anion, are capable of affecting the colour of metal ion solutions.

Highly conjugated organic compounds absorb light in the UV or visible regions of the electromagnetic spectrum. The solvents for these determinations are often water for water soluble compounds, or ethanol for organic-soluble compounds. The absorption spectrum of organic compounds may be highly affected by solvent polarity and pH.

While charge transfer complexes also give rise to colours, the colours are often too intense to be used for quantitative measurement [Skoog *et al.*, 1992]. Figure 2.15 illustrates how a UV-vis spectrometer functions.
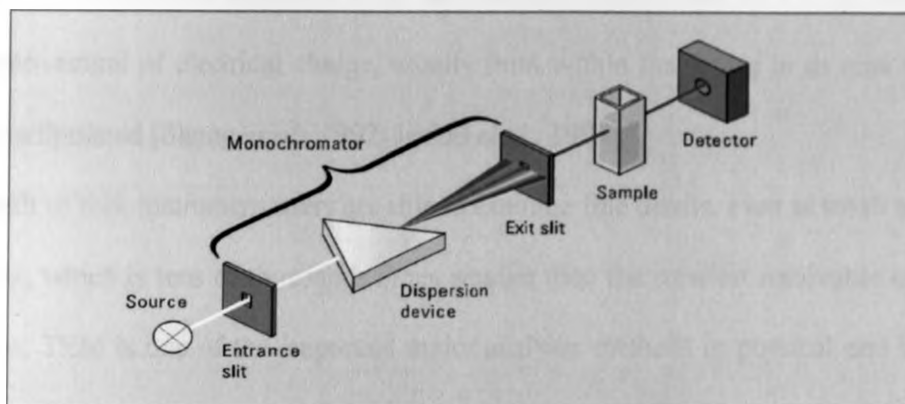
Figure 2.15: Schematic illustration of how a UV-vis spectrometer functions.

In a study by Arshi *et al.* (2011), silver/polyvinylpyrrolidone synthesized respectively in water and ethylene glycol were compared using UV-vis resulting in plasmon absorption peaks at 435 and 445 nm respectively. In another study by Hagedoorn *et al.* (2002), ferrous enzymes studied using UV-vis showed strong soret bands at approximately 409 nm. This value is characteristic of most heme enzymes such as CYP2E1.

2.6.6: Transmission Electron Microscopy (TEM)

Transmission electron microscopy (TEM) is a microscopic technique operational when a beam of electrons is transmitted through an ultra thin sample material, interacting with the sample as it passes through. The electrons behave as a light source with much lower wavelengths making it possible to obtain resolutions a thousand times better than using light microscopes. Depending on the density of the material present, some of the electrons are scattered and disappear from the beam, while at the bottom of the microscope the unscattered electrons hit a fluorescent screen, which gives

rise to a "shadow image" of the sample in question with its different parts displayed in varied darkness according to their respective densities. The interaction of the electrons with the sample create an image which is magnified and focused onto an imaging device, such as a layer of photographic film, a fluorescent screen or to be detected by a sensor such as a CCD camera (is a device for the movement of electrical charge, usually from within the device to an area where the charge can be manipulated [Skoog *et al.*, 1992; Jenkel *et al.*, 1994].

As a result of this, instrument users are able to examine fine details, even as small as a single column of atoms, which is tens of thousands times smaller than the smallest resolvable object in a light microscope. TEM is one of the important major analysis methods in physical and biological sciences finding application in virology, material science, and pollution, cancer and semiconductor research [Skoog *et al.*, 1992; Jenkel *et al.*, 1994]. The orientation of the instrument and its way of function is depicted below, figure 2.16 (A) and (B).

High voltage   A

Electron gun

First condenser lens

Condenser aperture
Second condenser lens
Condenser aperture
Specimen holder and air-lock
Objective lenses and aperture

Electron beam

Fluorescent screen and camera
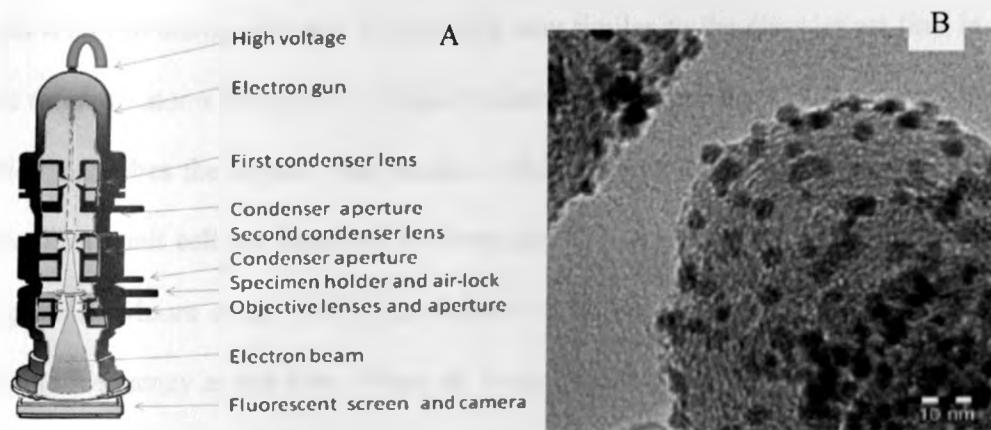
Figure 2.16: (A) Schematic presentation of transmission electron microscope (TEM) and (B) An example of a TEM image.

In this study TEM was used to study the morphology, shape, distribution and size of tea-AgNPs, PANI/tea-AgNPs nanocomposite, PANI film and PANI/tea-AgNP/CYP2E1 nanosensor.

2.6.7: Scanning Electron Microscope (SEM)

A scanning electron microscope is a type of electron microscope that images a sample by scanning it with a beam of electrons in a raster scan pattern. The electrons interact with the atoms that make up the sample producing signals that contain information about the sample's surface topography, composition, and other properties such as electrical conductivity [Russell *et al.*, 1985].

2.6.8: X-Ray Diffraction (XRD)

X-ray powder diffraction is most widely used for the identification of unknown crystalline materials (e.g. minerals, inorganic compounds), characterization of crystalline materials, identification of fine-grained minerals such as clays and mixed layer clays that are difficult to determine optically, determination of unit cell dimensions and measurement of sample purity. Solid matter can be described as amorphous or crystalline.

Amorphous refers to atoms arranged in a random way similar to the disorder we find in a liquid. Crystalline refers to atoms arranged in a regular pattern, and there is a smallest volume element that by repetition describes the crystal. The smallest volume element is called a unit cell (plane). The dimensions of the unit cell are described by three axes: a, b, c and the angles between them alpha, beta and gamma [Moore *et al.*, 1997]. An electron in an alternating magnetic field will oscillate with the same frequency as the field. When an X-ray beam hits an atom, the electrons around the atom start to oscillate with the frequency as the incoming beam. This model is complex to handle mathematically, and in day to day work we talk of about the X-ray reflections from a series of parallel planes in a crystal. The orientation and interplanar spacings of these planes are defined by the three integers of h, k, and l called indices. A given set of planes with indices h, k, and l cut a-axis of the unit cell in h sections, the b- axis in k sections and the c-axis in l sections. A zero indicates that the planes are parallel to corresponding axis. For instance: 2, 2, 0 planes cut a- and the

b-axis in half, but are parallel to the c- axis. International Center Diffraction Data (ICDD) or Joint Committee on Powder Diffraction Standards (JCPDS) is an organization that maintains the data base of inorganic and organic spectra. The data base is available from the Diffraction equipment manufacturers or ICDD direct. It is possible to calculate the particle size by using Scherrer's' formula and XRD patterns [Hou *et al.*, 2005].

2.6.9: Fourier-Transform Infrared Spectroscopy (FTIR)

Fourier Transform Infrared Spectroscopy (FTIR) is used for identifying types of chemical bonds in a molecule by producing an infrared absorption spectrum that is like a molecular "fingerprint". By interpreting the infrared absorption spectrum, the chemical bonds in a molecule can be determined. Molecular bonds vibrate at various frequencies depending on the elements and the type of the bond. For any given bond, there are several specific frequencies at which it can vibrate. According to quantum mechanics, these frequencies correspond to the ground state (lowest frequency) and several excited states (higher frequencies). One way to cause the frequency of a molecular vibration to increase is to excite the bond by having it absorb light energy. For any given transition between two states the light energy (determined by the wavelength) must exactly equal the difference in the energy between the two states [usually ground state (E_0) and the first excited state (E_1) [Griffiths *et al.*, 2007].

$$\text{Difference in Energy States} = \text{Energy of Light Absorbed}$$

$$E_1 - E_0 = h\,c\,/\,\lambda = h\nu$$

Where h = Planks constant
   c = Speed of light, and V= Velocity of light
   λ = Wavelength of light.

CHAPTER THREE: EXPERIMENTAL METHODOLOGY

3.1: Chemicals and solutions

Silver nitrate ($AgNO_3$), Aniline, Ammonium hydrate salt (97%), Cytochrome P450-2E1 Isozyme (CYP 2E10), Dihydrogenorthophosphate dehydrate, anhydrous and disodium hydrogenorthophosphate, Ethambutol [(2S, 2'S)-2, 2'-(ethane-1, 2-diyldiimino) dibutan-1-ol) - $C_{10}H_{20}N_2O_2$] were from Sigma-Aldrich and used as received. Analytical grade argon obtained from Afrox, SA. Tea leaves were from a local supermarket. Hydrochloric acid was supplied by Fluka. All chemicals were analytical reagent and were used as received. Solvent de-ionized ultra-purified water used throughout these experiments and was prepared with a Milli-Q water purification system.

3.2: Procedure for tea extract preparation

10 grams of tea powder was boiled to 90 °C in 100 ml of distilled water. The mixture was filtered through a normal filter paper and the filtrate centrifuged at 5000 rpm. The above procedure was repeated using 25, 30, 50 and 70 °C to demonstrate the effect of varying extraction temperature on the spectroscopic properties and particle size of the silver nanoparticles. The pH values of the extracts were recorded.

3.3: Procedure for 'Green' synthesis of Silver Nanoparticles (tea-AgNPs)

5mL of 1mM $AgNO_3$ solution was added to 10ml of tea extracts (supernatant). The solution was then hand shaken to ensure thorough mixing. The reaction was allowed to settle at room temperature. The procedure was repeated exactly as above using supernatant extracted at 25, 30, 50, and 70 °C. The pH values of the colloid were recorded.

3.4: Procedure for calculating Percent yield

The efficiency of the synthetic procedure in this work was determined by calculating the percent yield of the synthesized silvernanoparticles. At the final stage of the synthesis the product remained wet. As a result the sample was kept in an oven to let water evaporate out before weighing in order to avoid inflating the efficiency. The nanoparticles were dispersed in hexane to ensure that silver nanoparticles were not left behind at any stage during transfers. The nanoparticles were weighed and the mass recorded. The weight of Ag^0 was divided by the mass of Ag^+ ions in 1mM $AgNO_3$ making sure that both yields are in grams. The answer above was multiplied by 100 to get a final actual yield. This actual yield was expressed as a percentage of the theoretical yield;

$$\text{Percent yield} = \frac{\text{Mass of } Ag^0}{\text{Mass of } Ag^+} \times 100$$

3.5: Procedure for synthesis of Polyaniline (PANI)

The electropolymerization of aniline was performed in a cell solution containing 0.01 M of aniline monomer in 20 ml 0.1 M HCL solution degassed with argon for 15 minutes. The potential was cycled from -200 mV to +1000 mV, at a potential scan rate of 50 mV/s. An argon blanket was maintained on top of the cell solution during the polymerization process which was stopped after 5 voltammetric cycles. Polyaniline (PANI) was conditioned for biosensor application by rinsing out superficial acid and un-reacted monomer and then incubated in buffer. This electrode was referred to as Pt/PANI electrode.

3.6: Procedure for synthesis of Pt/PANI/tea-AgNPs

To develop the Pt/PANI/tea-AgNP electrode, 20 μl of tea- AgNPs dispersed in hexane were drop casted onto the Pt/PANI and allowed to dry at room temperature for one hour after which they were characterized using cyclic voltammetric technique at +1000 to -300 mV at various scan rates (5, 20, 30 50 and 100MV) in 0.1 M phosphate buffer, pH 7.4.

3.7: Procedure for Ultraviolet-Visible (UV-Vis) Spectrosphotometer

The Ultraviolet-Visible (UV-Vis) spectra for different samples (tea-AgNPs, PANI, and PANI/tea-AgNP) were recorded on a Nicolet Evolution 100 (Thermo Electron Cooperation, UK), and the samples were diluted five times before the study. The solution was put in a Quartz cuvette (1cm) and the solution run at a wavelength range of 250 to 900nm.

i. The instrument was switched on and left to initialize for about 10 minutes.

ii. Baseline correction was done using deionised water as the blank and the instrument was set to run between the wavelengths of 250 to 900 nm.

iii. Cuvettes were cleaned using deionised water.

iv. The instrument was run and the spectra recorded and saved in a computer.

v. The procedure was repeated for all the samples and this was also repeated during the stability studies.

For monitoring the formation of the nanoparticles as a function of time, the absorption of the sample was recorded as they formed without diluting until saturation was reached. For tea-AgNPs, three different spectra were recorded. To compare the effect of extraction temperature, the spectra of silver nanoparticles synthesized using tea molecules at (a) 25, (b) 30 (c) 50 (d) 70 and (e) 90 °C were recorded. To monitor the formation of the silver nanoparticles as a function of time, the

absorption spectra of a solution containing 1 mM Ag ions was taken at different times (in minutes): 0, 20, 30, 40, 50, 60, 120 and 300 minutes. The supernatant extracted at 25 °C was preferred since it was easy to handle and it was for comparison purposes. And finally, UV-vis spectra of supernatant tea broth, mixture of supernatant tea broth and $AgNO_3$ and silver nanoparticles were recorded in order to compare their spectra. The supernatant extracted at 90 °C was preferred since it gave well defined and larger peaks than others.

3.8: Procedure for Transmission Electron Microscope

Morphological studies of tea-AgNPs were carried out using transmission electron microscopy (TEM). Three samples of AgNPs extracted at 25, 70 and 90 °C were studied using this technique. A drop of each sample (dispersed in hexane) was placed over carbon-coated standard copper grids and allowed to dry prior to measurements. TEM images were acquired on Philips Technai-FE 12 TEM instrument operated at an accelerating voltage of 120 kV. The instrument was equipped with an Energy dispersive X-ray (EDAX) detector (Oxford LINK-ISIS 300) for elemental composition analysis and the EDAX spectra were measured at an accelerating voltage of 10 Kv. 316 AgNPs samples were randomly chosen from the micrographs and the average particle size was estimated recorded.

3.9: Procedure for Scanning Electron Microscope (SEM)

Tea-AgNPs, PANI, and PANI/tea-AgNPs samples were studied using SEM. Images were taken with a Hitachi S3000N scanning electron microscope at an acceleration voltage of 20 kV at various magnifications. Gold sputtering of the SEM samples was done using a SC7640 Auto/

Manual high resolution super coater (Quorum Technology Ltd., England) at a voltage of 2 kV and plasma current of 25 mA for one minute. The modified Pt/PANI/tea-AgNPs/CYP2E1 electrodes were used for the detection of TB drug.

3.10: Procedure for X-Ray Diffraction

The XRD characterization was used to determine the crystal structure of silver solids synthesized and to determine the effect of tea extracts on the crystallization. Samples were dried before the analysis. A PANanalytical Xpert Pro θ-2θ diffractometer using Cu Kα radiation at 45 kV and 40 mA was used. Scans were typically in the range 2θ = 20- 85 °C, with 0.02^0 step sizes that were held for 2 seconds each. Pattern analysis was performed using the Jade+ software v.7 or later (MDI Inc., Livermore, CA), which generally followed the ASTM D934-80 procedure. Reference patterns were from the 2002 PDF-2 release from the ICDD (International Center for Diffraction Data, Newtown Square, PA). Open-circuit voltage potentials were obtained using 1 M NaCl with reference to a saturated calomel electrode (SCE) [Moore *et al.*, 1997].

3.11: Procedure for Fourier Transform Infrared Spectroscopy (FTIR)

The lattice vibrational behaviour of tea extract before and after reduction of the Ag ions was studied with the FTIR in order to probe the possible molecules in tea extract responsible for the reduction and capping of the Ag ions. The extract after complete reduction of Ag+ was centrifuged at 12000 rpm for 20 minutes to isolate the silver nanoparticles from other compounds present in the solution. FTIR spectra were obtained using a Nicolet Magna-IR system 560 FTIR spectrometer at room temperature. Sample for FTIR were prepared by dropping a sample between two plates of sodium chloride (salt) and analyzed in a liquid cell. This is a small container made from NaCl

which can be filled with liquid, such as the extract for EPA 418.1 analysis. This creates a longer path length for the sample, which leads to increased sensitivity. Sampling methods included making a mull of a powder with hydrocarbon oil (Nujol) to cast a film [Chamberain *et al.*, 1969].

3.12: Procedure for cyclic voltammetry

All electrochemical experiments were carried out using a BAS 100W integrated automated electrochemical workstation BioAnalytical Systems (BAS, West Lafayette, IN) controlled by a computer and a conventional three-electrode system with a 0.0201 cm^2 gold (Au) disk or screen printed gold electrode (SPAuE) as the working electrode, a platinum (Pt) wire auxillary electrode and Ag/AgCl reference electrode with a 3 M NaCl salt bridge solution, all purchased from (BAS, West Lafayette, IN). All the results obtained for the PANI, PANI/Tea-AgNPs and [PANI/Tea-AgNPs/CYP2E1 using cyclic (CV), differential pulse (DPV) square wave (SWV) voltammograms and steady state amperometry (constant potential amperometry) were recorded with a computer interfaced to the electrochemical workstation. Alumina micropolish (1.0, 0.3 and 0.05 mm alumina slurries) and polishing pads (Buehler, IL, USA) were used for polishing the electrode. All experiments were done at room temperature (20- 25 $^\circ$C).

Cyclic voltammetry (CV) characterization of the PANI, PANI/Tea-AgNP and PANI/Tea-AgNPS/CYP2E1 modified electrodes were carried out at a potential window of -1000 mV (initial potential, E_i) to +1000 mV (switch potential, E_λ), sensitivity of 10 μA/V and at different scan rates (5 – 100 mV/s). The modified electrodes were also investigated using Differential Pulse Voltammetry (DPV). The DPV experimental conditions were: potential window of +1000 mV to -1000 mV, sensitivity of 10 μA/V, pulse amplitude of 50 mV, current sampling width of 17 msec, pulse width of 50 msec and at different scan rates (10 – 200 mV/s). Characterization of the modified electrodes was also carried out using Square Wave voltammetry (SWV). SWV experimental

conditions were: potential window of +1000 mV to -1000 mV, sensitivity of 10 μA/V, SWV amplitude of 25 mV.

i. The electrochemical cell was washed with deionised water and rinsed thoroughly.

ii. Electropolymerization was achieved by the use of aniline, ammonium hydrate salt 97% in the polymerization medium, hydrochloric acid.

iii. The nanobiosensors were prepared using, Cytochrome P450-2E1 Isozyme (CYP 2E1).

iv. The enzyme was stored at -4 °C under anhydrous conditions when not in use.

v. The reaction medium, pH 7.4, 0.1 M phosphate buffer was prepared from dihydrogenorthophosphate dehydrate, anhydrous and disodium hydrogenorthophosphate.

vi. Analytical grade argon was used for degassing the cell solutions and all the solutions were kept refrigerated at -4 °C when not in use.

3.13: Preparation of Pt/PANI/Tea-AgNP/CYP2E1 Nanobiosensors

A freshly prepared Pt/PANI/tea-AgNPs electrode was reduced at a constant potential of -650 mV for 600 seconds under an argon blanket in a 2 ml solution of buffer until a steady state current was attained which took 5 minutes to attain. 20 μl of CYP2E1 was added to a 2 ml solution of 0.1 M phosphate buffer, and the Pt/ PANI/tea-AgNPs nanocomposite was oxidized at a potential of +650 mV for 2 minutes during which the PANI/tea-AgNPs nanocomposite was electrostatically attached with CYP2E1. The resultant PANI/tea-AgNPs/CYP2E/nanobiosensor was rinsed in buffer to remove excess enzyme and stored refrigerated at -4 °C when not in use.

3.14: Application of PANI/Tea-AgNP/CYP2E1 Modified Pt Electrodes

The experiment was carried out at room temperature. The modified electrodes [Pt/PANI/Tea-AgNPs/CYP2E1] were tested for the amperometric sensing of ETH (the TB drug). Standard solution was prepared daily by dissolving 0.0014g of ETH in 50 mL phosphate buffer resulting in final concentrations of ETH = 0.001 M ETH. Different concentrations of the drug were varied independently in 20 ml of phosphate buffer solutions. The volumetric determination of these drugs was carried out in 20 ml phosphate buffer under the following techniques; Cyclic voltammetric (CV) experiments were carried out at a potential window of +1000 mV to -1000 mV, sensitivity of 10 µA/V and at 20 mV/s at different concentrations of the drug and the DPV experimental conditions were: potential window of +1000 mV to -1000 mV, sensitivity of 10 µA/V, pulse amplitude of 50 mV, current sampling width of 17 msec, pulse width of 50 msec and at 50 mV/s at different concentrations of the drug; while the SWV experimental conditions were: potential window of +1000 mV to -1000 mV, sensitivity of 10 µA/V, SWV amplitude of 25 mV. Data obtained from DPV and SWV detection experiments was not included as the data was not consistent even after several trials of changing the working parameters.

3.15: Stability and reproducibility

The stability and reproducibility of the Pt/PANI/Tea-AgNPs/CYP2E1 nanobiosensor was investigated in pH 7.4, 0.1 M phosphate buffer solution for two weeks and the modified bioelectrodes were stored at 4 °C when not in use. Ten successive detection measurements of ETH, was carried out for two weeks.

CHAPTER FOUR: RESULTS AND DISCUSSION

4.1: Preparation of tea extracts

Preliminary studies with tea extracts of different brands gave similar results. Rooibois (grown in the region of Western Cape Province of South Africa) tea extracts were used for the reported results in the present work. Although there was no direct determination of freely extractable phenolic compounds in rooibos tea extracts namely (-)-epigallocatechin-3- gallate (EGCG), (-)-epigallocatechin (EGC), (-)-epicatechin-3- gallate (ECG), and epicatechin (EC), it was possible to detect their presence through a change in colour intensity of the resultant solution, which increased with increase in extraction temperature. Moreover, the pH values also varied with the change in temperature as indicated in table 4.1, further suggesting their presence. These compounds are slightly acidic as seen from the pH values, further supporting their presence. The extent of acidity increases with increase in temperature and this indicates that the extraction efficiency increased with increase of extraction temperature.

Table 4.1: pH values of aqueous tea extract corresponding to extraction temperature (Accuracy of the pH meter: +/- 0.05).

Extraction temperature (^{o} C)	pH Values
25	5.36
30	5.35
50	5.33
70	5.31
90	5.30

4.2: Preparation of silver nanoparticles using tea extracts (tea-AgNPs)

On adding silver nitrate solution to aqueous tea extracts at room temperature in a ratio of 1:2 (volume by volume), the solution instantaneously turned from water colour to pale yellow and

then dark brown (figure 4.1) indicating the formation of metallic silver nanoparticles [Nadagouda et al., 2010].
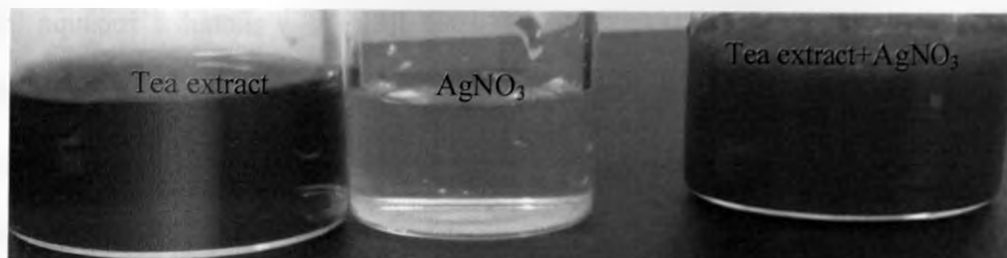
Figure: 4.1: Colour changes indicating formation of AgNPs using AgNO$_3$ and tea extracts

The pH values of the colloidal silver nanoparticles synthesized using tea bio-molecules extracted at 25, 30, 50, 70 and 90 °C are shown in table 4.2. The acidity is due to the presence of tea bio-molecules on the surface of AgNPs. Tea extracts alone have a higher pH values compared to a mixture of tea extracts and AgNPs.

Table 4.2: pH values of colloidal silver nanoparticles (Accuracy of the pH meter: +/- 0.05).

Extraction temperature of tea extracts (° C)	pH Values of colloidal silver nanoparticles
25	4.39
30	4.38
50	4.36
70	4.34
90	4.33

4.3: Percent yield of tea-AgNPs

To calculate percent yield, the mass of Ag$^+$ ions reacting with tea extract was calculated. 5ml of AgNO$_3$ was added to 10ml of tea extract during the synthesis. The atomic mass of elemental

-51-

silver is universally known to be 107.8682 g. Out of the total five atoms present in $AgNO_3$, Ag contributes one atom It then follows that, from the total number of atoms and atomic mass of $AgNO_3$, percent mass of Ag was calculated to be 63.449%. Further, mass of Ag^+ ions in 1000ml and 5ml aqueous solutions was calculated to be 0.10722881 g and 0.0005 g due to 200 times dilution respectively. Thus the mass of Ag^+ present in the solution for reduction by tea extracts (at extraction temperature of 90 degrees) was 0.005 g. Tea-AgNPs synthesized weighed 0.004 g. The percent yield was therefore calculated by dividing the mass of AgNPs by the mass of Ag^+ ions in 5ml aqueous solution [John Olmsted, *et al.*, 2006]. The percent yield of AgNPs was calculated to be 80 ± 0.5 % (table 4.3). This means that 80 ± 0.5 % of the product would be recovered if the reaction were 100 % efficient.

Ag^+ ions acquire an electron from tea extracts and are reduced to Ag^0. Percentage yield was calculated in order to determine the efficiency of the synthetic procedure. This calculation was done for other extraction temperatures; 25, 30, 50 and 70 °C (See Appendix). The percent yield increased with increase in extraction temperatures, indicating that more AgNPs were synthesized at 90 °C. Even though, the calculated yield is not excellent, it is acceptable. Losses in the nanoparticles may be attributed to the centrifuging process to separate the nanoparticles from the extract and some nanoparticles could have remained in the supernatant. Also, some might have accidentally spilled over during transfers. To improve the yield, the nanoparticles were dissolved in hexane so that none of the particles remained on the tube during transfers. Further, the nanoparticles were dried before weighing to avoid inflating the results. Although, there could be likely traces of impurities on the surface of the silver nanoparticles, there is no reported method of calculating the present quantities.

Table 4.3: Calculation of percent yield of AgNPs corresponding to 90 °C.

A tomic mass of Ag, g	-	107.8682 g
Number of Ag atoms Present in AgNO₃.	-	1
Mass percent of Ag in AgNO₃,	$\dfrac{107.8682}{169.9 \text{ (Mass of AgNO}_3)} \times 100$	63.489%
Mass of Ag⁺ in 0.169 g of AgNO₃ (1mM) dissolved in 1000 ml distilled water (stock solution), g.	$\dfrac{63.489}{100} \times 0.169$	0.10729641 g
Mass of Ag⁺ in 5 ml aqueous solution of the 1000 ml aqueous solution, g.	$\dfrac{5* 0.107229641}{1000}$	0.0005 g
Mass of tea-AgNPs synthesized (Weighed), g.	-	0.0004 g
Percent yield	$\dfrac{0.0004 \text{ g}}{0.0005 \text{ g}} \times 100$	80%

4.4: Electrosynthesis of polyaniline (PANI) on platinum electrode (Pt/PANI)

PANI was grown on a 0.0201 cm² disk electrode surface in an acidic medium by the potentiodynamic oxidative polymerisation of 0.01 M aniline in 0.5 M HCL at 50 mV/s scanning anodically from –200 to +1000 mV versus Ag-AgCl. Figure 4.2 shows a typical cyclic voltammogram of the polymer film on Pt produced after 5 voltammetric cycles. The peaks A, B and C are reduction peaks (i.e. gain of an electrons) whereas A', B' and C' are oxidation peaks (i.e. loss of electrons).

-53-
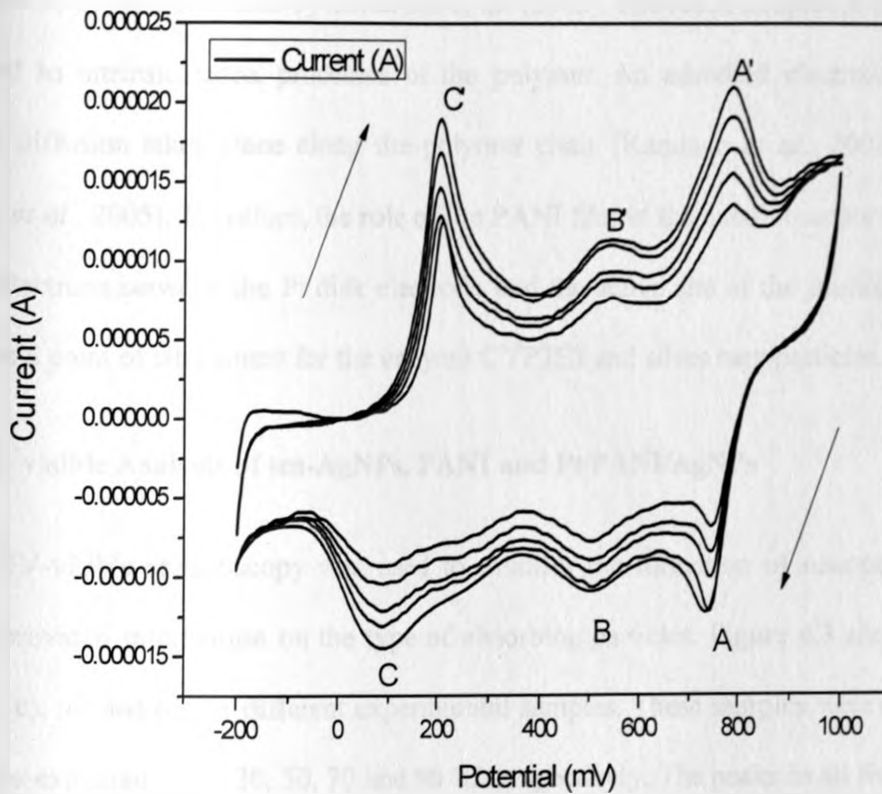
Figure 4.2: Cyclic voltammogram of the polymer film on Pt electrode produced after 5 voltammetric cycles.

It can be seen that upon polymerization, PANI possesses three redox couple which is consisted with the works of Iwuoh et al. (1997) and Mathebe et al. (2004). Oxidation of aniline on already deposited polymer involves charge transportation across the polymer film and is therefore energetically more demanding, whereas the reduction of the accumulated polymer film becomes easier.

Only results of cyclic voltammetric characterization at 50 mV/s are included in this work, since characterizations at different scan rates (10, 20, 30, 40, 50, 70, 80, 90 and 100 mV/s) of PANI in the presence of the polymerization acidic media showed similar electrochemistry as denoted by

the configuration of their peaks. The characterization of PANI shows a similar electrochemistry to that of PANI in the work done by Lindofors *et al.* (2002). The redox couples A'/A B'/B and C'/C are attributed to intrinsic redox processes of the polymer. An adsorbed electroactive polymer with electron diffusion takes place along the polymer chain [Kanungo *et al.*, 2002; Mu *et al.*, 1997; Bistolas *et al.*, 2005]. Therefore, the role of the PANI film in the nanobiosensor construction was to shuttle electrons between the Pt disk electrode and the active site of the immobilized enzyme and served as a point of attachment for the enzyme CYP2E1 and silver nanoparticles.

4.5: UV- visible Analysis of tea-AgNPs, PANI and Pt/PANI/AgNPs

UV-visible spectroscopy was used to monitor the formation of nanoparticles. UV-visible spectra provided information on the type of absorbing particles. Figure 4.3 shows spectra labeled (a), (b), (c), (d) and (e) for different experimental samples. These samples were made from tea bio-molecules extracted at 25, 30, 50, 70 and 90 °C, respectively. The peaks in all five spectra appeared to be wide with double peaks. The most intense peaks were located at ca. 451 nm, 450nm, 450 nm, 450 nm and 450 nm, respectively and the other peak which was less intense was located at ca. 350 nm. The sample extracted at 90 °C showed the highest peak. Sample extracted at room temperature (25 °C) showed the smallest peak intensity. The peak intensity increases as the extraction temperature is increased suggesting presence of a higher number of absorbing particles, attributable to increased amount of extracts and extraction efficiency. A very similar behavior is noted in the works of Begum et al., (2009). AgNPs are known to absorb radiation in the visible region (ca. 380-450 nm) [Huang *et al.*, 2004]. The absorbance has a general shift towards the shorter wavelengths (blue shift) suggesting formation of particles with smaller diameters as extraction efficiency is improved.
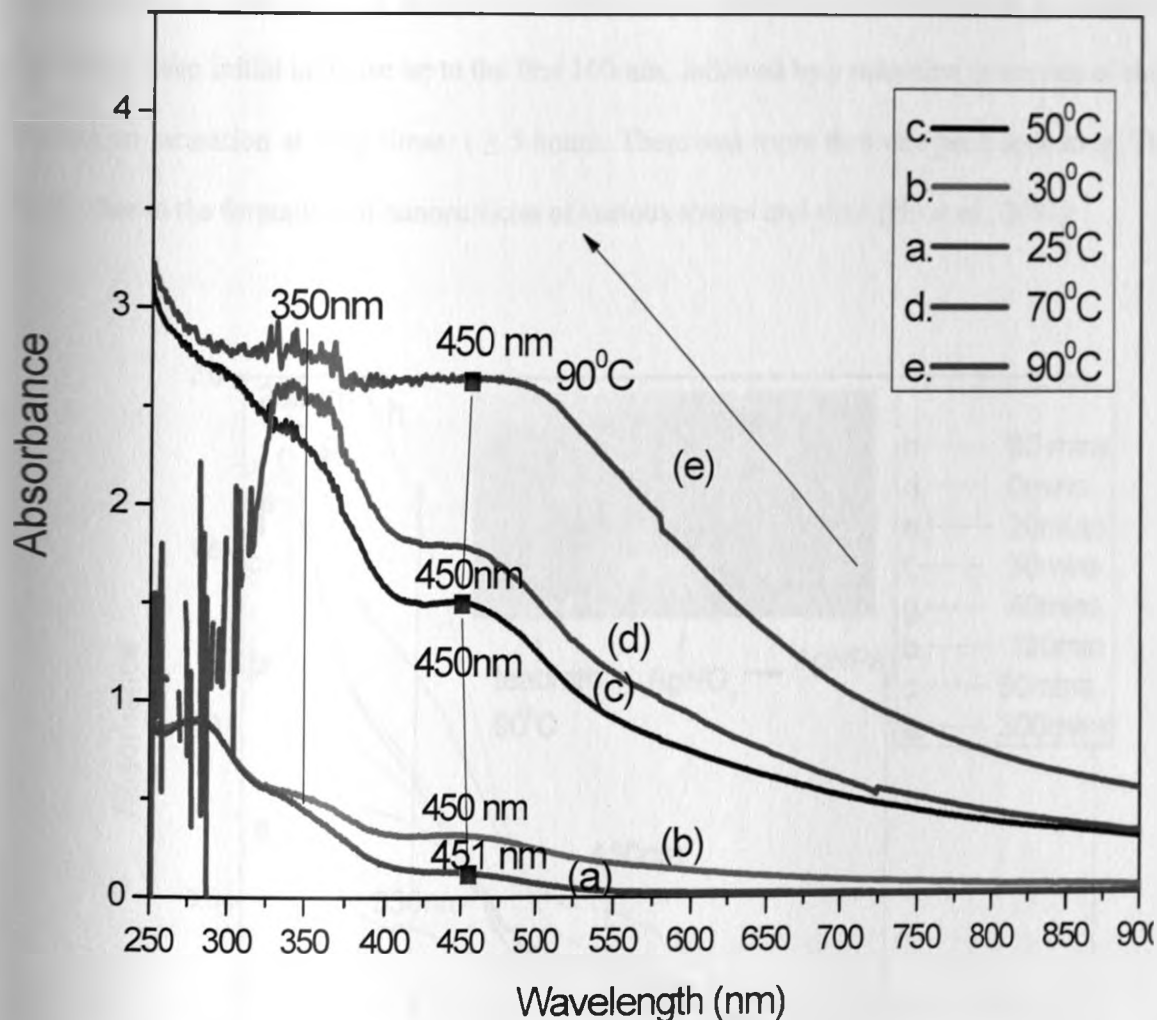
Figure 4.3: UV-vis Spectra of silver nanoparticles synthesized using tea leaves extract at (a) 25, (b) 30 (c) 50 (d) 70 and (e) 90 °C. The peaks at ca. 451, ca. 450, ca. 450, ca. 450 and ca. 450 nm correspond to the surface plasmon resonance of silver nanoparticles at 25, 30, 50, 70 and 90 °C, respectively.

The progress of the reaction between silver ions and the tea leaf extracts were monitored by recording the absorption spectra as a function of time. Figure 4.4 shows the result of the reaction between Ag^{I} containing-solutions and the tea extracts. At t= 0 minutes i.e., at the instant of addition of Ag^{I} solution, the absorption spectrum of the reaction media showed a low peak suggesting that

nanoparticles formed instantly and solution turned from light-brown to dark brown. The absorbance showed a steep initial increase up to the first 100min, followed by a reduction in the rate of change, leading to saturation at long times: $t \geq 5$ hours. There was more than one peak appearing. This is likely due to the formation of nanoparticles of various shapes and sizes [He *et al.*, 2002].
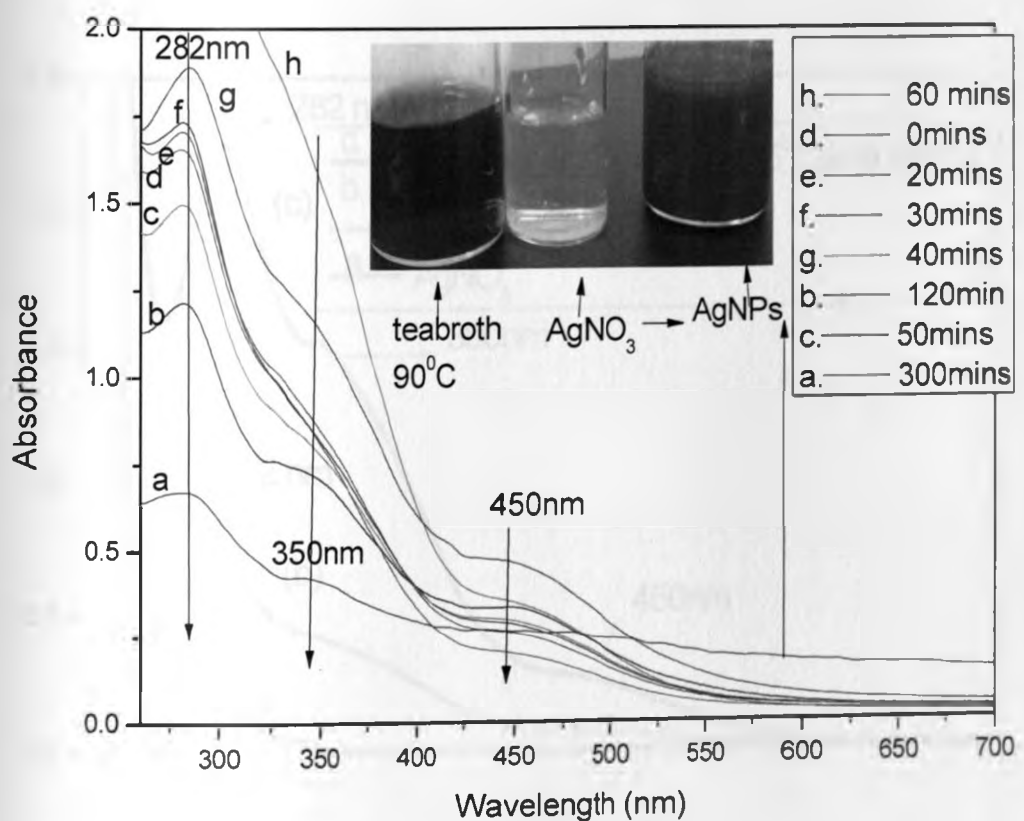
Figure 4.4: Absorption spectra of a solution containing 1 mM Ag ions in tea media taken at different times (in min): 0, 20, 30, 40, 50, 60, 120 and 300min, as indicated by different colours. Inset shows the colour changes as the nanoparticles form.

The absorbance of tea extracts was compared with that of AgNO$_3$ solution and a mixture of AgNO$_3$ solution and tea extracts. Figure 4.5 represents the absorption spectrum of AgNO$_3$ solution denoted by 'a', tea extracts denoted by 'b' and mixture of tea extracts and AgNO$_3$ solution denoted

-57-

by 'c'. Tea extracts showed absorption at ca. 282 nm while AgNO₃ solution did not show any absorption. A mixture of tea extracts and AgNO₃ solution showed absorptions at ca. 282 nm, ca. 350 nm and ca. 450 nm. The absorption at ca. 350 and ca. 450 nm is attributed to the absorption of AgNPs whereas absorption at ca. 282 nm is attributed to the absorption of tea bio-molecules on the surface of AgNPs.
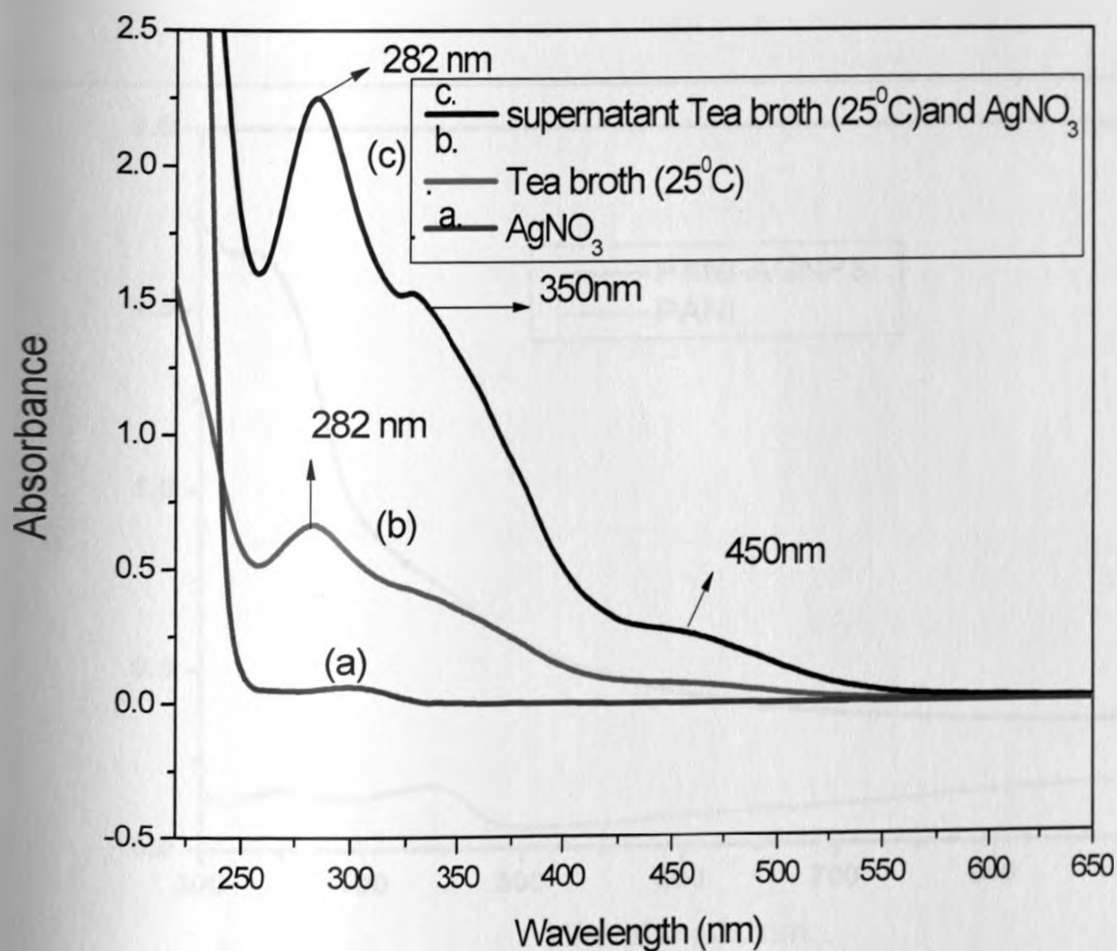
Figure 4.5: UV-Vis Spectra of AgNO₃ (a), Tea both (b) and Mixture of supernatant Tea broth and AgNO₃ (c) at (25 °C).

UV-vis spectroscopy was also used to evaluate PANI and PANI-Tea-AgNPs (figure 4.6). Two distinct peaks were observed at 370 nm and 450 nm. These peaks are attributed to $\pi - \pi^*$ transition of benzoid rings and are indicative that nanostructed PANI showed the formation or the presence of the stable pernigraniline salt. Depending on their specific location, the presence of these peaks is either associated with charge transfer excitons of the quinoid structure or due to the doping level [Iwuoha et al., 2006].
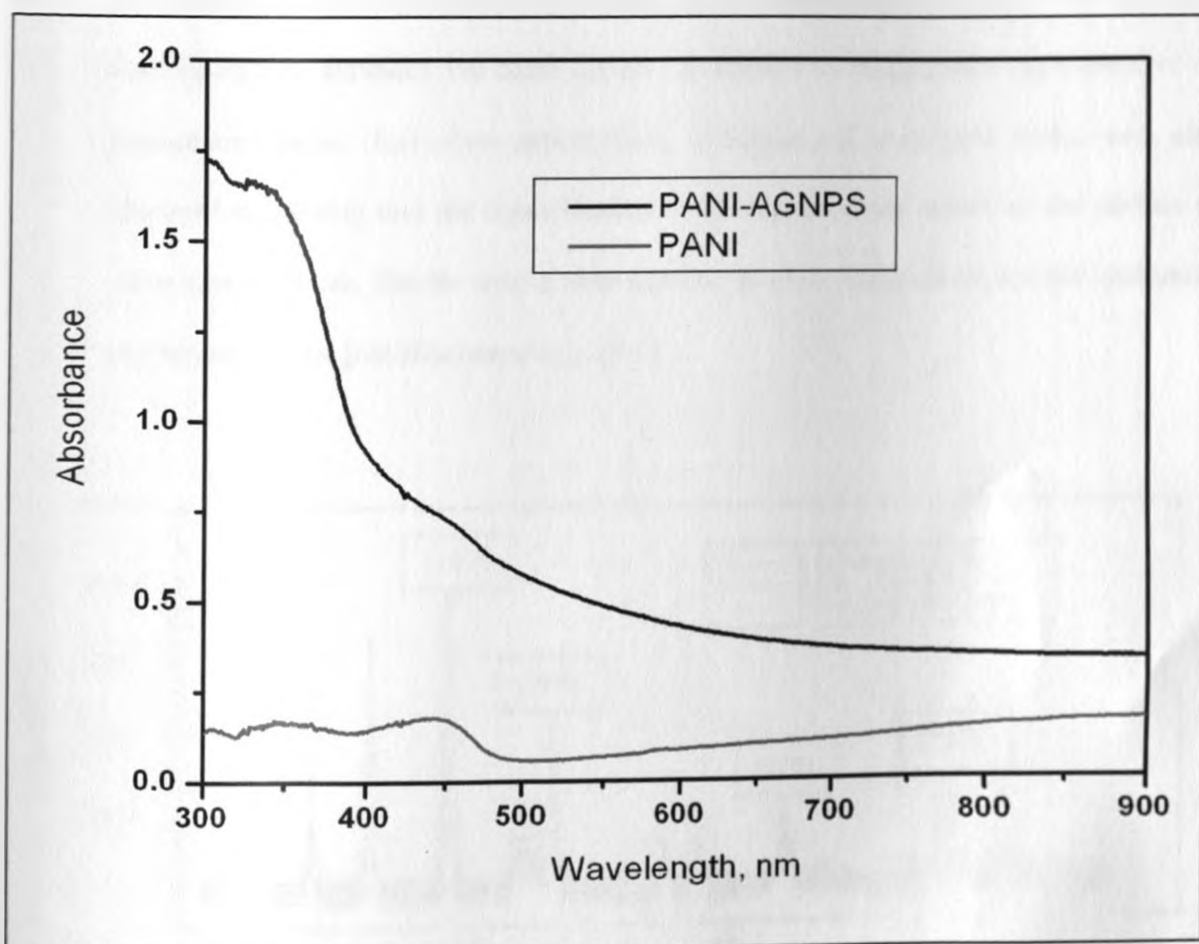
Figure 4.6: UV-visible spectroscopy of PANI and PANI/tea-AgNPs

4.6: X-Ray Diffraction (XRD) study of tea-AgNPs

Crystalline nature of Ag nanoparticles was confirmed from XRD analysis. Figure 4.7 shows the XRD patterns of AgNPs obtained corresponding to extraction temperatures of tea extract (25, 70 and 90 °C). Four peaks were observed at (38.21, 44.31, 64.71, 77.81 and 82.51), under the diffraction angle $2\theta = 35$- 80 °C and can be indexed to the (111), (200), (2 20) and (321) planes which corresponds to the four faces of silver cube crystal according to the standard specimen [Owen. E. A. Williams, G. I. J. Sci. Instrum. 04-0783]. This indicates that tea-AgNPs exhibited the cubic crystal. In addition to Bragg peaks representative of face-centred cubic (fcc) silver nanocrystals, additional and unassigned peaks were also observed suggesting that the crystallization of bio-organic phase occurs on the surface of silver nanoparticles. Similar results were reported in silver nanoparticles synthesized using mushroom extract [Mallikarjuns *et al.*, 2011].
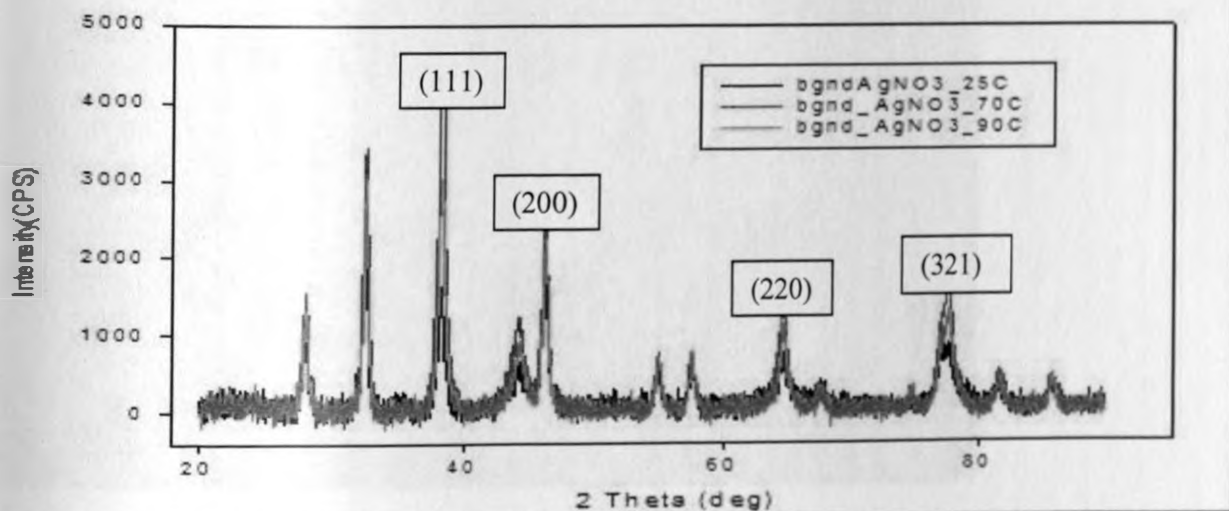
Figure 4.7: X-Ray Diffraction (XRD) patterns of the prepared nanoparticles. Labeled peaks correspond to the characteristic diffraction peaks of elemental Ag (0).

4.7: Transmission Electron Microscope (TEM) study of tea-AgNPs

High resolution transmission electron microscope (HRTEM) study of tea-AgNPs revealed primarily spherical nanoparticles that were polydispersed. Particles with various sizes were synthesized corresponding to extraction temperatures: for tea extracted at 90 °C, the primary larger particle was measured to be 10 nm with a smaller primary particle size of 2 nm and average particle size of 4.4 nm (figure 4.8 and table 4.4).

Figure 4.8: Spherical and polydispersed tea extract synthesized AgNPs using 90 °c as the extraction temperature of water (black spots) embedded in the tea matrix.

Table 4.4: particle size distribution of tea extract synthsized AgNPs using 90 °C as the extraction temperature randomly obtained from micrograph.

Particle size, nm	Frequency	Percent
2.00	73	23.1
3.00	18	5.7
4.00	96	30.4
5.00	36	11.4
6.00	63	19.9
8.00	20	6.3
10.00	8	2.5
Total	316	100.0

For tea extracted at 70 °C, the primary larger particle was measured to be 20 nm with a smaller primary particle size of 2 nm and average particle size of 4.78 nm (figure 4.9 and table 4.5).

Figure 4.9: Spherical and polydispersed tea extract synthesized AgNPs using 70 °C as the extraction temperature of water (black spots) embedded in the tea matrix.

Table 4.5: particle size distribution of tea extract synthsized AgNPs using 70 °C as the extraction temperature randomly obtained from micrograph.

Particle size, nm	Frequency	Percent
2.00	80	25.3
2.50	28	8.9
3.00	35	11.1
4.00	63	19.9
5.00	18	5.7
6.00	22	7.0
8.00	24	7.6
10.00	38	12.0
20.00	6	1.9
Total	316	100.0

For tea extracted at 25 °C, the primary larger particle was measured to be 25 nm with a smaller primary particle size of 2 nm and average particle size of 5.7 nm (figure 4.10 and table 4.6).
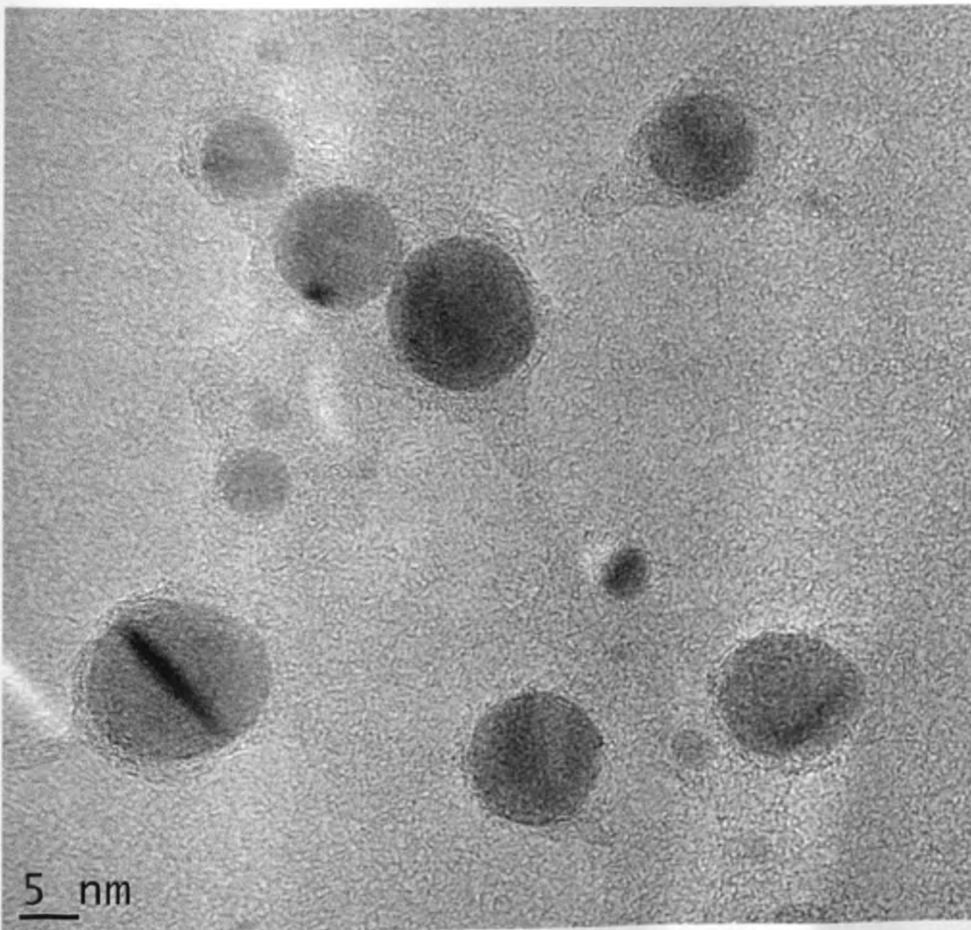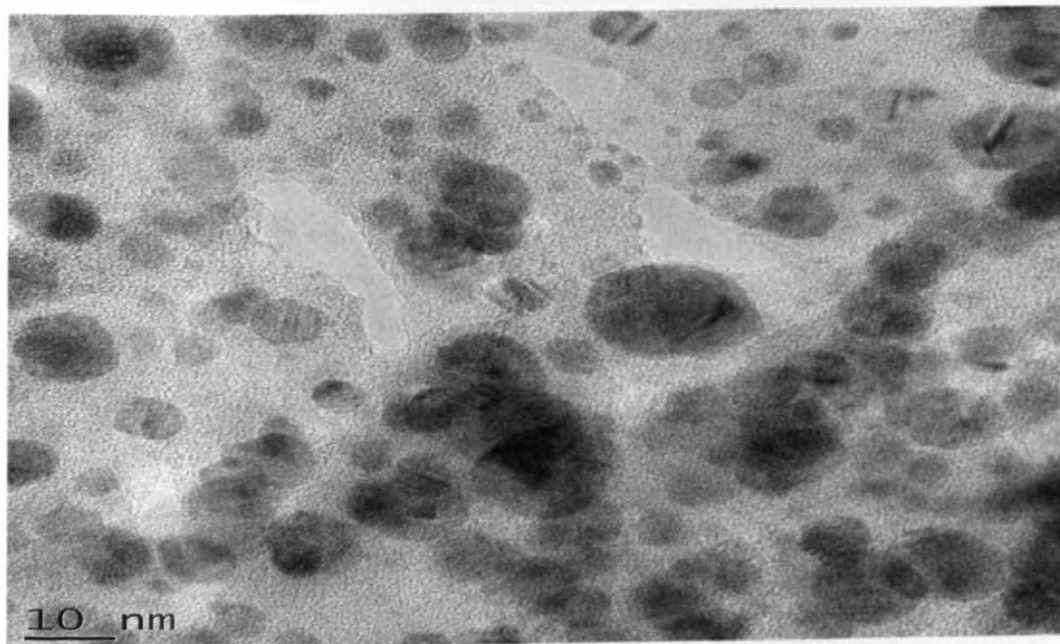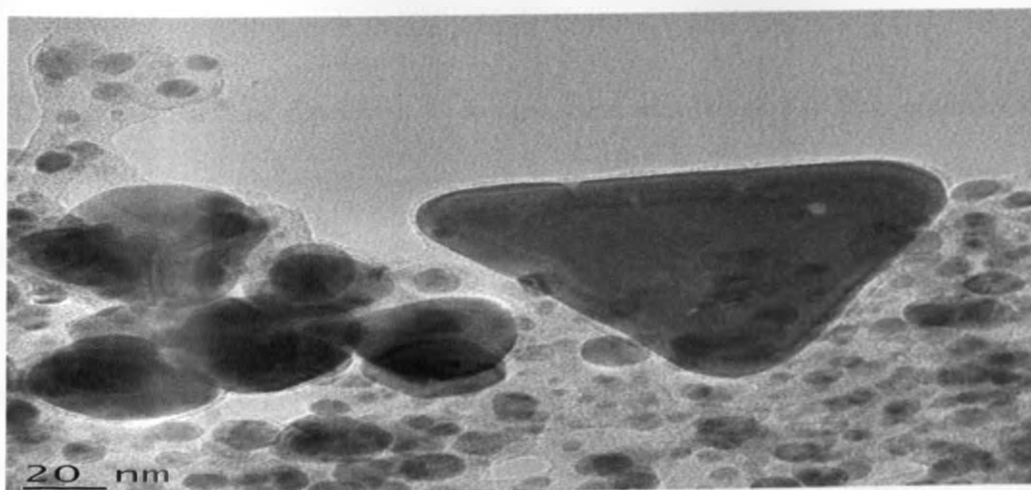

Figure 4.10: Spherical and polydispersed tea extract synthesized AgNPs using 25 °C as the extraction temperature of water (black spots) embedded in the tea matrix.

Table 4.6: particle size distribution of tea extract synthsized AgNPs using 25 °C (extraction temperature).

Particle size, nm	Frequency	Percent
2.00	60	19.0
2.50	25	7.9
4.00	41	13.0
5.00	61	19.3
6.00	31	9.8
7.00	1	.3
8.00	33	10.4
10.00	56	17.7
20.00	5	1.6
25.00	1	.3
Total	316	100.0

The variation in size distribution is in agreement with the shift in their absorbance peaks. The shift of maximum absorption wavelength with increasing extraction temperature may be attributed to overall dimunition of the particle size. In some cases, it seemed more likely that two or more particles were situated close to each other, rather than a single particle. From HRTEM micrographs it is seen that bio-molecules are present among the particles and are adhered to their surfaces.. Average particle size decreased with increasing extraction temperature. This implies that the presence of large quantity of tea extracts cause strong interaction between protective biomolecules and surface of nanoparticles preventing nascent nanocrystals from sintering. With larger quantities of the extract the interaction is intensified, leading to size reduction of spherical nanoparticles. With low quantities of tea extract, reduction of silver ions was fulfilled, but failed to

protect most of the quasi-spherical nanoparticles from aggregating. Further, the HRTEM showed AgNPs to be crystalline as can be seen from the selected diffraction pattern area recorded from one of the nanoparticles (figure 4.11).
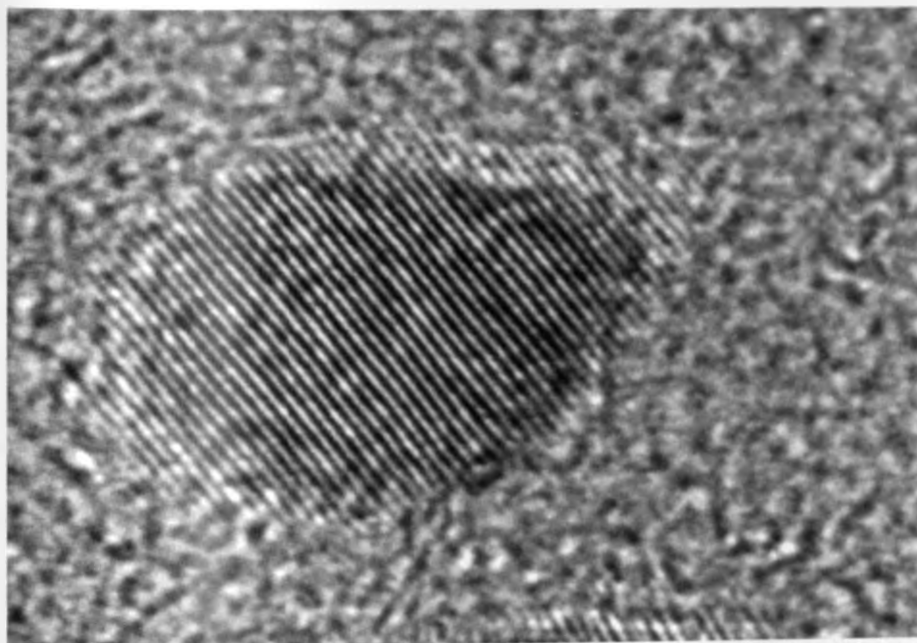
Figure 4.11: Layers of equal distance on the TEM image of one of the nanoparticles showing fringe lattice of the crystalline nature of the synthesized silver nanoparticles.

4.8: Energy Dispersive X-ray Analysis (EDX)

EDX analysis (figures 4.12 to 4.14) indicated in all cases that the main constituent element was Ag. Other elemental signals were also recorded namely; carbon, oxygen and copper. Carbon and oxygen signals are possibly due to emissions from bio-molecules present in the tea extracts while copper is a result of the copper grid onto which the nanoparticles were immobilization for TEM analysis [Kumar *et al.*, 2011].
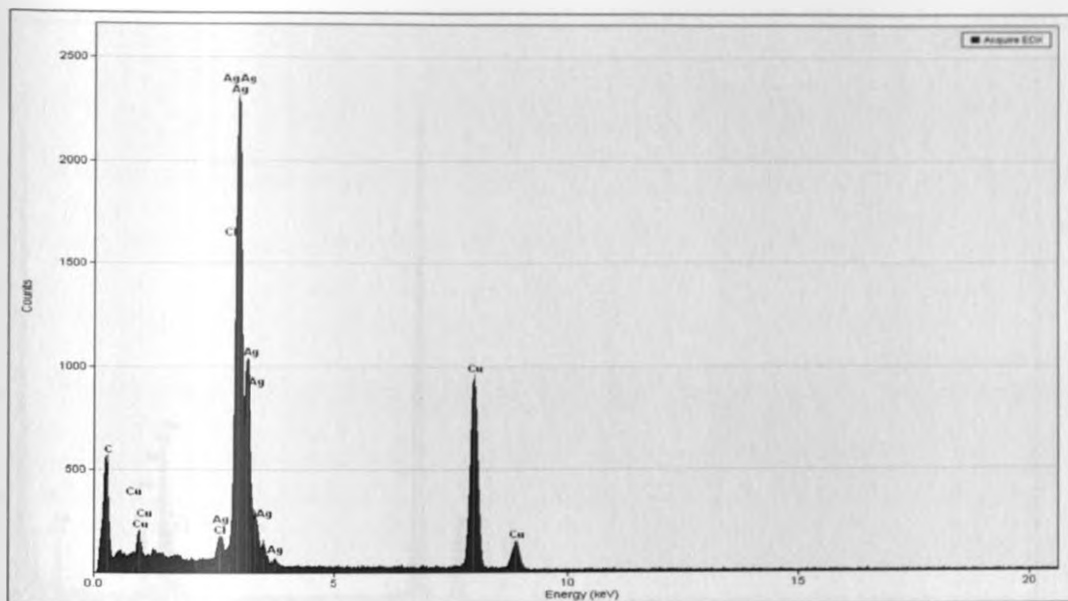
Figure 4.12: Energy Dispersive X-ray (EDX) spectrum of spherical and polydispersed tea extracts synthesized AgNPs using 90 °C as the extraction temperature of water. Different x-ray emission peaks are labeled.
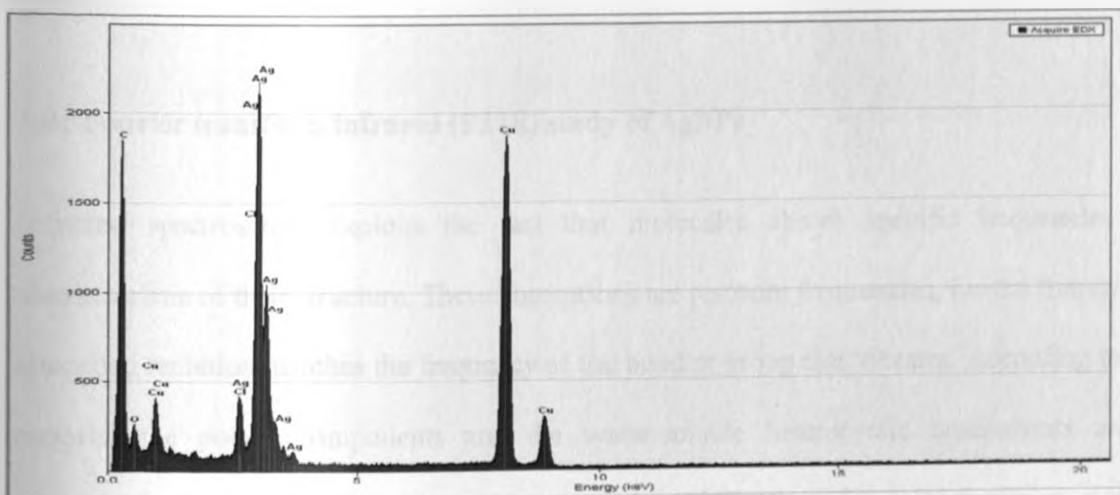
Figure 4.13: Energy Dispersive X-ray (EDX) spectrum of Spherical and polydispersed tea extract synthesized AgNPs using 70 °C as the extraction temperature of water. Different x-ray emission peaks are labeled.
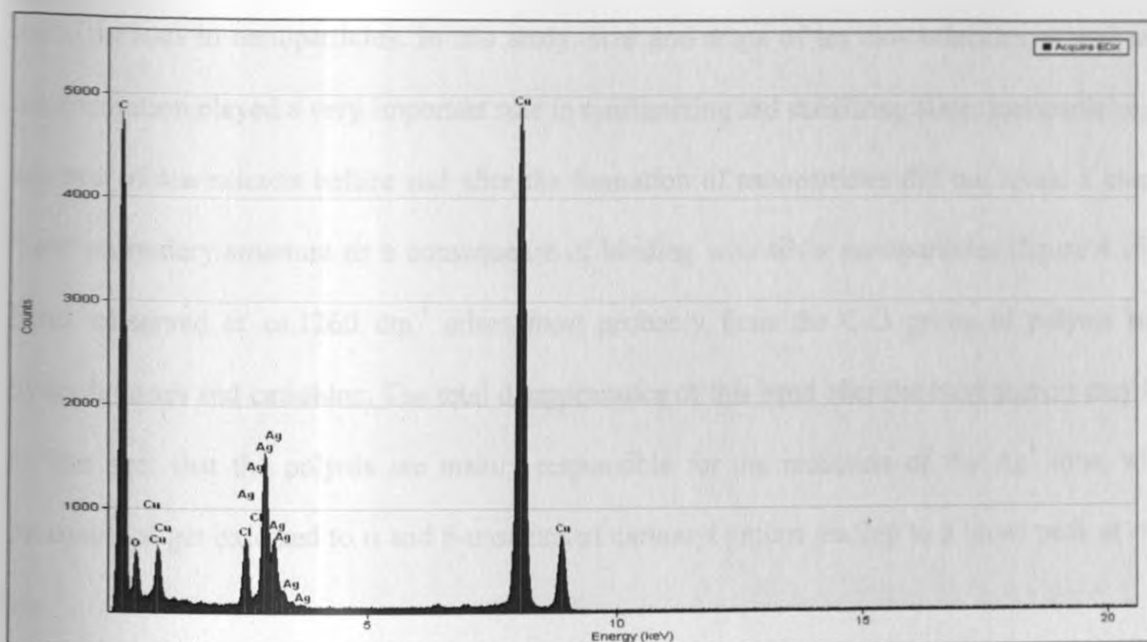
Figure 4.14: Energy Dispersive X-ray (EDX) spectrum of Spherical and polydispersed tea extract synthesized AgNPs using 25 °C as the extraction temperature of water. The different x-ray emission peaks are labeled.

4.8: Fourier transform infrared (FTIR) study of AgNPs

Infrared spectroscopy exploits the fact that molecules absorb specific frequencies that are characteristic of their structure. These absorptions are resonant frequencies, i.e. the frequency of the absorbed radiation matches the frequency of the bond or group that vibrates. According to previous reports, the polyol components and the water-soluble heterocyclic components are mainly responsible for the reduction of metal ions and the stabilization of the nanoparticles, respectively. There are also reports on reductases (Ahuja *et al.*, 2007) and polysaccharides (Huang and Yang, 2004) as factors involved in biosynthesis and stabilization of the nanoparticles, respectively.

Tea biomolecules largely polyphenols are rich in polyols and donate electrons which reduce the metallic ions to nanoparticles. In this study, size and shape of tea bio-molecules as well as their conformation played a very important role in synthesizing and stabilizing silver nanoparticles. FTIR spectra of tea extracts before and after the formation of nanoparticles did not reveal a change to their secondary structure as a consequence of binding with silver nanoparticles (figure 4.15). The band observed at ca.1260 cm^{-1} arises most probably from the C-O group of polyols such as hydrolavones and catechins. The total disappearance of this band after the bioreduction may be due to the fact that the polyols are mainly responsible for the reduction of the Ag$^+$ ions, whereby themselves get oxidized to α and β-unsaturated carbonyl groups leading to a broad peak at ca.1650 cm^{-1}.
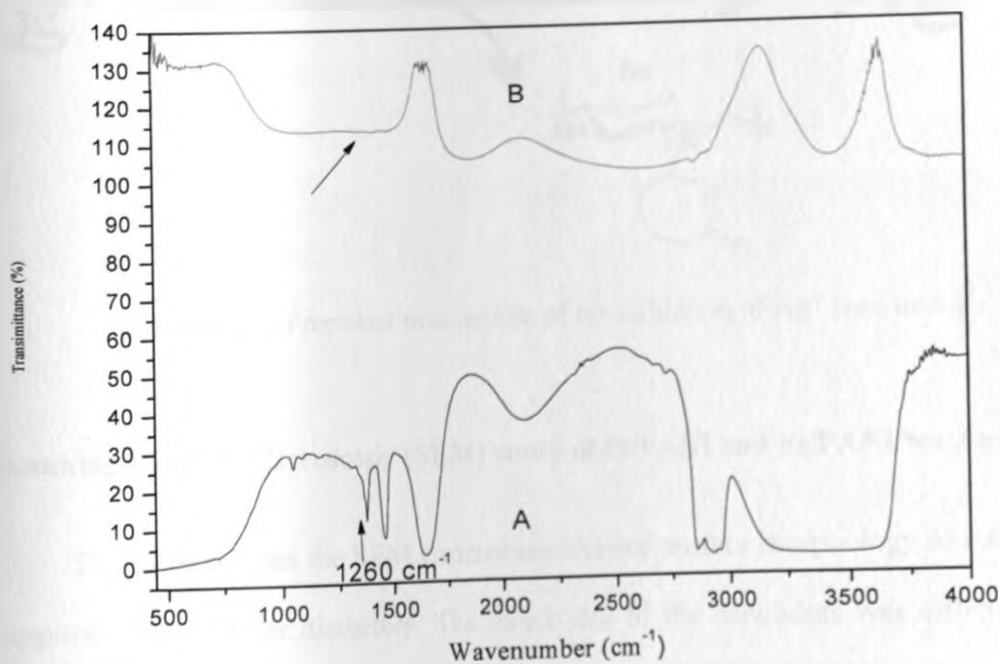
Figure 4.15: Fourier transform infrared (FTIR) spectra of tea extracts before (A) and after (B) formation of AgNPs.

The silver ion reduction as a result of electrons donated by tea extracts induces the formation of a lactone moiety on the polyphenol (Fetizon reaction) without causing C–C bond cleavage on the polyol. The close and multivalent arrangement of the endogenous reducing agent (alditols) on the polyphenols backbone resulted in the formation of silver nanoparticles. The proposed mechanism of this oxidation is illustrated in scheme 4.1. [Donati *et al.*, 2009].
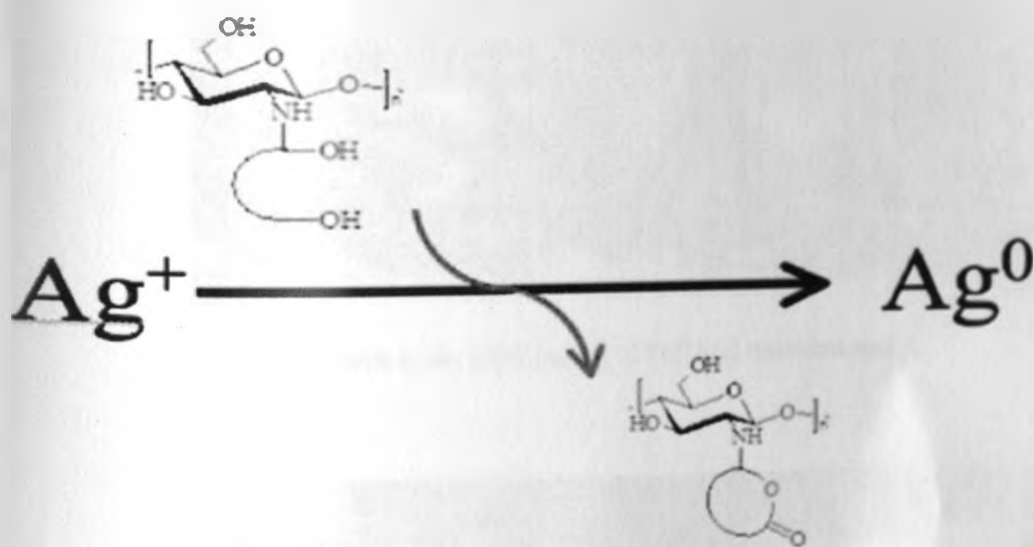
Scheme 4.1: Proposed mechanism of the oxidation of Ag$^+$ ions to Ag^0.

4.9: Scanning Electron Microscopy (SEM) study of Pt/PANI and Pt/PANI/tea-AgNPs

The pictures from the SEM experiment showed surface morphology of PANI nanotubes with approximately similar diameters. The exact size of the nanotubes was difficult to measure because of the rough resolution of the pictures. Figure 4.16 shows the SEM morphology film where regular and uniform PANI nanotubes are observed. Their network structure increased the effective surface area of the electrode. The layer-by-layer nanotubes observed for the morphology of PANI

was seen to cover the electrode surface allowing the adsorption of silver nanoparticles. Figure 4.17 gives the SEM image of tea-AgNPs drop coated onto PANI (PANI/tea-AgNPs nanocomposite). The tea-AgNPs are seen to cover the Pt/AgNPs surface allowing the adsorption of enzyme.
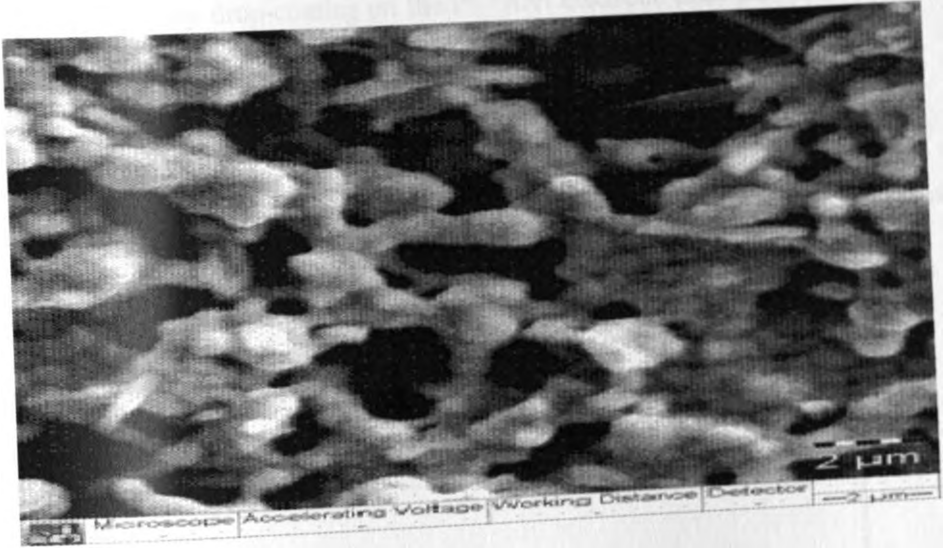
Figure 4.16: SEM image of Pt/PANI nanocomposite.
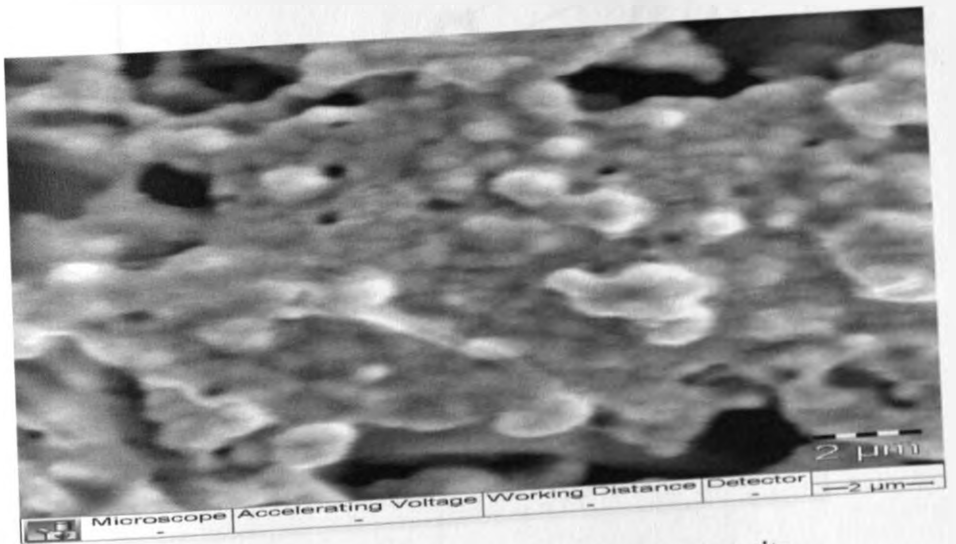
Figure 4.17: SEM image of Pt/PANI/tea-AgNPs nanocomposite.

4.10: Voltammetric study of tea-AgNPs, PANI/tea-AgNPs and PANI/tea-AgNPs/CYP2E1

The effect of the tea-AgNPs on the electroactivity of PANI was evaluated by comparing the profile of the three electrodes namely; Pt/PANI, Pt/Tea-AgNPs and Pt/PANI/Tea-AgNPs. 20 µl of tea-AgNPs were deposited by drop-coating on the Pt/PANI electrode after polymerization of PANI and allowed to dry at room temperature for 1 hour.

Modification of PANI by tea-AgNPs on the electrode surface was accompanied by a large background current from the Ag (I) to Ag (0) transition indicating that the electroactive area of Pt electrode has been increased due to the high special surface area of tea-AgNPs (figure 4.18).
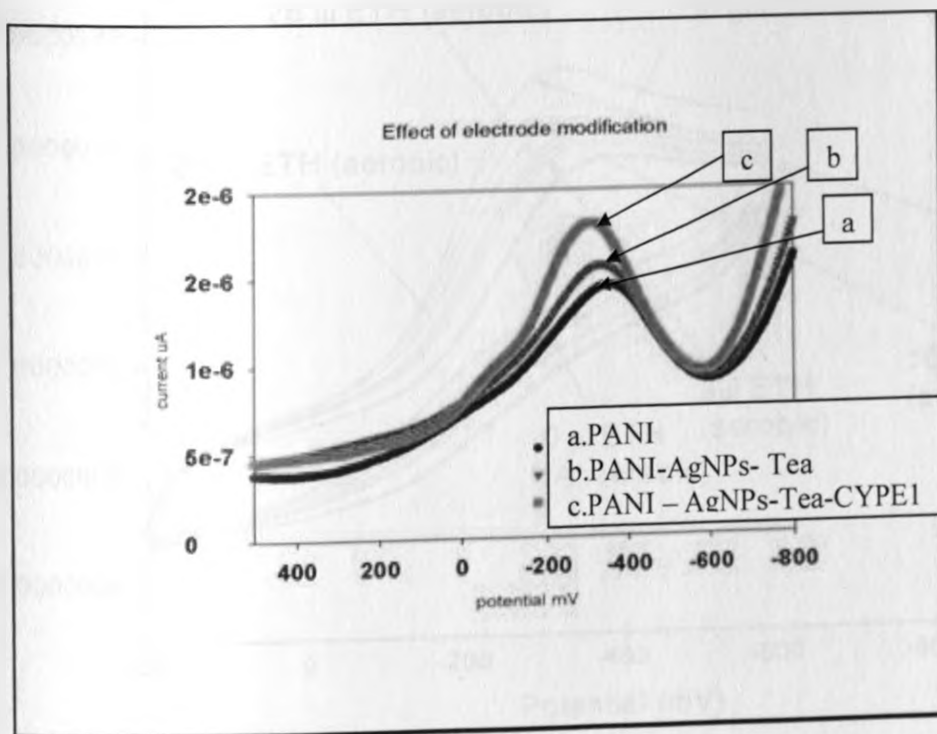
Figure 4.18: Voltammetric study of tea-AgNPs, PANI/tea-AgNPs and PANI/tea-AgNPs/CYP2E1.

Application of PANI/tea-AgNPs/CYP2E1 nanobiosensor in the electrocatalytic reduction of Ethambutol

The electrocatalytic activity of CYP2E1 in the PANI/Tea-AgNPs nanocomposite was evaluated by cyclic voltammetry technique (CV). Pt/PANI/Tea-AgNPs/CYP2E1 was employed as the working electrode and its electrochemical response towards ethambutol (ETH) investigated in 0.1 M phosphate buffer, pH 7.4, under aerobic conditions at scan rate of 20 mV/s. In the absence of ETH, electrocatalytic activity of CYP2E1 in the PANI/Tea-AgNPs nanocomposite was evaluated by CV method under anaerobic conditions figure (4.19).
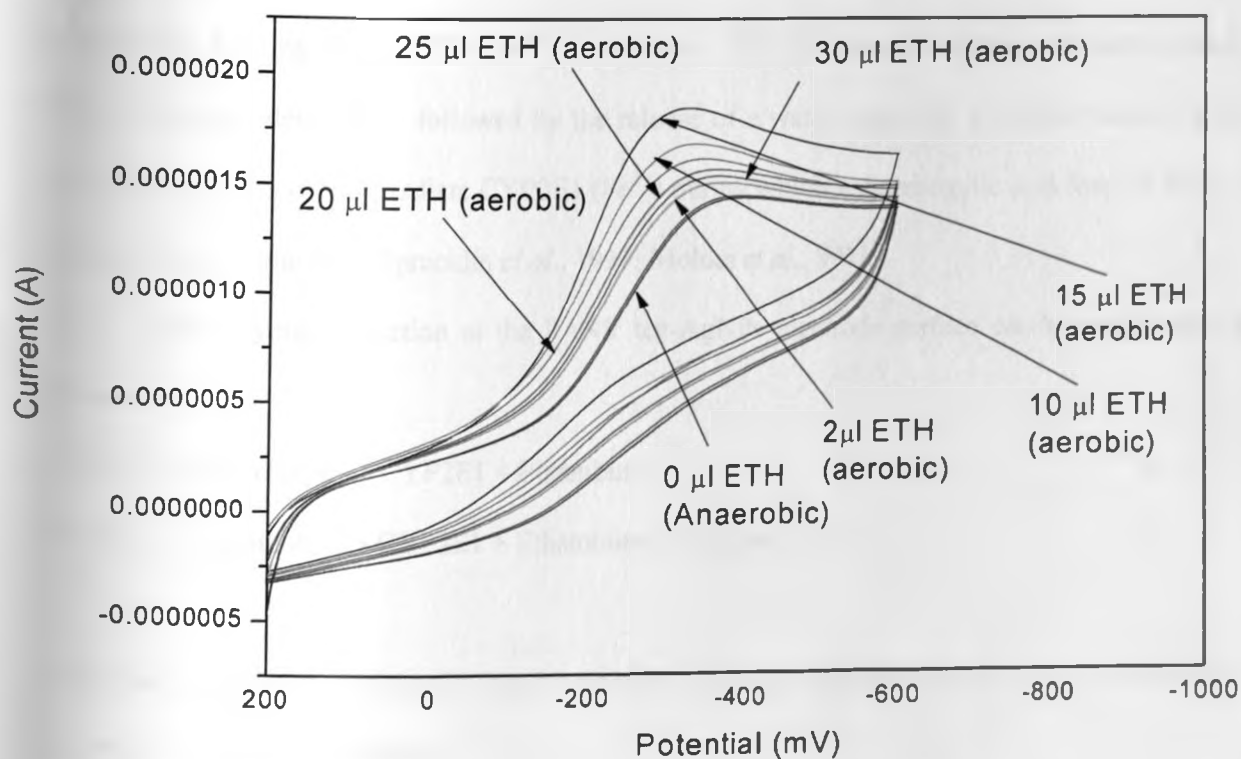
Figure 4.19: PANI/tea-AgNPs/CYP2E1 nanobiosensor in the electrocatalytic reduction of Ethambutol (ETH).

When 2 μl of ETH was injected into the buffer reaction medium under anaerobic conditions, the reduction peak increased with a corresponding oxidation peak observed. It means that the CYP2E1 enzyme interacted with the ETH analyte reductively and the process being predominantly non-reversible. Subsequent injections of aliquots of ETH saw an increase of current until saturation was reached at 20 μl when current started to drop. In the absence of analyte, electroactivity of CYP2E1 was evaluated under anaerobic conditions, where we only have the electrochemistry of Pt/tea-PANI/CYP2E1 which is essential for the oxidation and of PANI and tea-AgNPs respectively.

The reduction peak observed in aerobic conditions suggests the one electron electrochemical reduction of hexa-coordinated low-spin ferric enzyme (Fe^{3+}) to high spin ferrous enzyme (Fe^{2+}). This form of the enzyme has a high affinity for oxygen and thus binds molecular oxygen present in the solution forming the CYP2E1 (Fe^{2+}) O_2 complex. This interaction resulted in the development of an aldehyde intermediate followed by the release of a water molecule. The result was a highly active iron-oxoferryl intermediate CYP2E1 (Fe^{4+}) during which a dicarboxylic acid form of ETH is produced upon reduction [Spracklin et al., 1997; Moltke et al., 997].

The enzymatic reaction at the PANI/ tea-AgNPs electrode surface can be considered as follows:

CYP2E1 + Ethambutol → CYP2E1 – Ethambutol   K₁

CYP2E1 – Ethambutol → CYP2E1 + Ethambutol Aldehyde + H_2O K₂
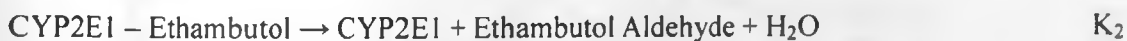
Therefore, based on the Michaelis-Menten reaction, the enzymatic kinetics of CYP2E1 as shown in scheme 4.2 is written as follows:

$$V = K_2 [CYP\,2E1][ETHAMBUTOL\quad]/\,K_M + [ETHAMBUTOL\quad]$$

Where V is the rate, K_2 the equilibrium constant, K_M the Michaelis-Menten constant, [CYP2E1] the concentration of CYP2E1 and [ETHAMBUTOL] is the concentration of ethambutol.

Naturally, lower K_M and higher V values are preferred since they indicate a high enzyme biocatalytic activity. At lower ETH concentrations, the rate of reaction is directly proportional to the ETH concentration. Therefore, when $V = V_{MAX}$ then K_M is numerically equal to half the ETH concentration.

The blood peak level of ethambutol ($1 - 5$ µg/mL) or $6 - 18$ µM occurring between $4 - 8$ hr post a daily dosage of 200 mg, is within the dynamic linear response range ($2 - 18$ µM). With an upper dynamic linear range of 18 µM it means that the nanobiosensors are effective and can be applied to systems where concentrations are 0.7 µM - 18 µM. Scheme 4.2 shows a proposed reaction scheme showing the metabolism of ethambutol using the Pt/PANI/Tea-AgNPs/CYP2E1 nanobiosensor.
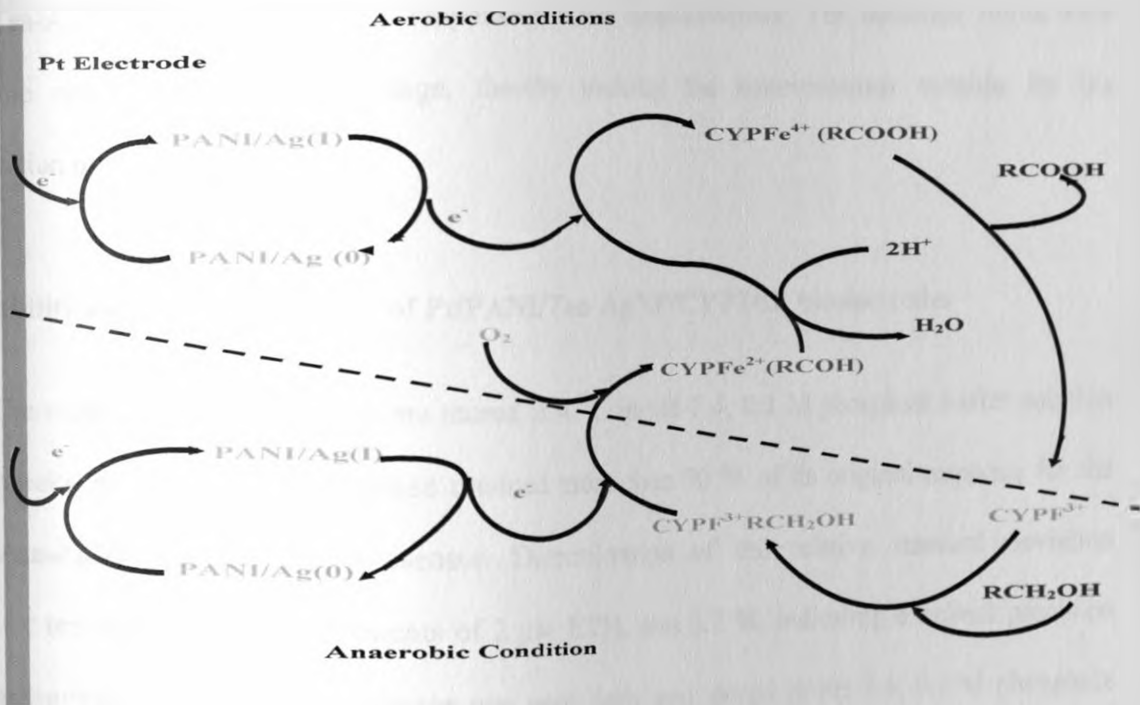
Scheme 4.2: Proposed reaction scheme showing the metabolism of ethambutol using the Pt/PANI/Tea-AgNPs/CYP2E1 nanobiosensor.

KEY: CYP$^{4+, 3+, 2+}$ – Different oxidation states of Cytochrome P450-2E1

PANI/Ag – PANI/ silver nanoparticle nanocomposite

RCH$_2$OH – Ethambutol
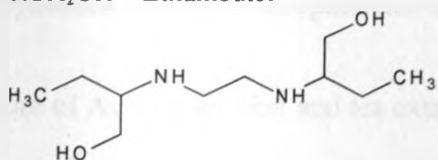
RCOH – Ethambutol aldehyde intermediate
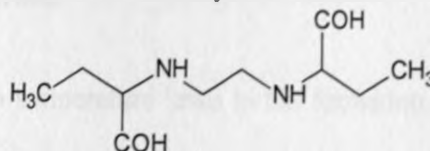
COOH – Dicarboxylic acid ethambutol
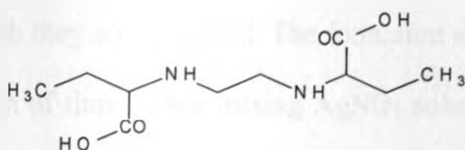
Tea-AgNPs enhanced current response for the nanobiosensor. The detection limits were within the nanobiosensor linear range, thereby making the nanobiosensor suitable for the determination of respective analytes.

4.12: Stability and Reproducibility of Pt/PANI/Tea-AgNP/CYP2E1, bioelectrodes

The modified bioelectrodes were stored at 4 ^{0}C in pH 7.4, 0.1 M phosphate buffer solution for two weeks, and the current response retained more than 90 % of its original response for the Pt/PANI/tea-AgNP/CYP2E1 nanobiosensor. Determination of the relative standard deviation (R.S.D) for ten successive measurements of 2 µM ETH, was 3.2 %, indicating excellent precision for the measurement. The nanobiosensor was used daily and stored in pH 7.4. 0.1 M phosphate buffer solution at 4 ^{0}C when not in use. The data received from these experiments indicated that the current responses only decreased by an average of less than 15 % suggesting that the nanobiosensors reported for this work have long-term stability (two weeks).

CHAPTER FIVE: CONCLUSIONS AND RECOMMENDATIONS

5.1: Conclusions

5.1.1: Synthesis of Silver nanoparticles using tea extracts

A mixture of $AgNO_3$ solution and tea extracts at room temperature leads to the formation of silver nanoparticles. Shape and size of the nanoparticles is dependent on the concentration of the tea extract and $AgNO_3$ solution used. The concentration of tea extract is dependent on the temperature at which they are extracted. The formation of silver nanoparticles is instantaneous and builds up as function of time. Upon mixing $AgNO_3$ solution and tea extracts at room temperature, the mixture turns from water colour to pale yellow and then to dark brown indicating the formation of the nanoparticles. The synthetic procedure is highly efficient as evidenced by a percent yield of 80 ± 0.5%.

5.1.2: Characterization of tea-AgNPs

The UV- visible spectra of silver nanoparticles synthesized using tea extracts (tea-AgNPs) show an absorption at ca. 450 nm and 350 nm. The absorption peak shifts to longer wavelengths (red shift) with decreasing concentration of tea extracts, as a result of decreasing extraction temperatures. Thus, the efficiency of tea extracts towards synthesis of silver nanoparticles increases with extraction temperature. The tea-AgNPs exhibits a cubic crystal and as Transmission Electron Microscopy (TEM) results show, they are spherical, polydispersed with size ranging between ca. 2-20 nm.

5.1.3: Application of tea- AgNPs in nanobiosensors.

PANI drop coated with AgNPs is highly electroactive. The resulting Tea-AgNPs/ PANI nanocomposite can be successfully coated on Platinum electrode to provide a platform for immobilization of the enzyme CYP2E1. The Tea-AgNPs/PANI nanocomposite serves as a point of attachment for the enzyme as well as an efficient electron mediator between the redox centre of CYP2E1 and the electrode surface. The result obtained confirms that the Pt/Tea-AgNPs/PANI/CYP2E1 nanobiosensors are successful and can be applied in the reductive catalysis of the TB drugs into respective water soluble and easy excretable metabolites. The nanobiosensor has a stability of two weeks and the detection limits were found to be within the nanobiosensor linear range, thereby making the nanobiosensor systems suitable for the determination of the respective analytes in serum.

5.2: Recommendations

Based on the conclusions made from the results of the current research work, the following are the recommendations for further work:

1. More applications to the biosynthesized nanoparticles.

2. Need to determine the optimum extraction temperature of tea extracts for the synthesis of silver nanoparticles which are monodispersed.

3. More research work needs to be done to establish the detailed expected reaction of tea extract with the silver nitrate solution.

4. More work needs to be done to determine polyphenols in tea extracts which are responsible for the reduction of the Ag ions to Ag^0.

5. The applications of tea-AgNPs in the current work covered only Ethambutol drug, based on the results obtained, there is need to extend the application of Pt/PANI/Tea-AgNPs/CYP2E1 to other TB drugs namely, Isoniazid (INH), Rifampin (RIF) and Pyrazinamide (PYR).

6. More research needs to be done to improve specificity and selectivity of the nanobiosensors in order to discriminate more efficiently between closely related forms of tuberculosis treatment drugs or other compounds which could be biotransformed using these systems.

REFERENCES

Adhikari B. and Majumdar S. (2004). *"Polymers in sensor application,"* Progress in Polymer. Vol. **29**, 700-701.

Ahuja T. and Kumar D. (2009). *"Recent progress in the development of nano-structured conducting polymers/nanocomposites for sensor applications,"* Sensors and Actuators B. Vol. **136**, 275-276.

Ahuja T., Mir I. A. And Kumar D. (2007). *"Biomolecular immobilization on conducting polymers for biosensing application,"* Biomaterials, Vol. **28**, 791-794.

Alqudami A., Annapoorni S., Sen P. And Rawat R.S. (2007). *"The incorporation of silver nanoparticles into polypyrrole: Conductivity changes,"* Synthetic Metals, Vol. **157**, 53-54.

Anastas P. T., Heine L. G. and Williamson T. C. (2000). *"Green Chemical Syntheses and Processes,"* ACS Symposium Series, Vol. **767**; American Chemical Society: Washington, DC, 1-6.

Anastas P.T. and Warner J. C. (1998). *"Green Chemistry:* Theory and Practice.Oxford University Press, Inc. New York.

Arshi N., Ahmed F., Koo B. H. and Lee C. G. (2011). *"Camparative study of the Ag/PVP nanocomposites synthesized in water,"* Current Applied Physics, Vol. **11**, 347-348.

Bennett P. N. and Brown M. J. (2007). *"Clinical Pharmacology"* Tenth Edition, Churchill Livingstone Elsevier Ltd: Spain, 219-222.

Bistolas N., Wollenberger U., Jung C. and Scheller F.W. (2005). *"Cytochrome P450 biosensors a review"* Biosensors and Bioelectronics, Vol. **20**, 2409-2411.

Bhamkar D.R., Joshi H.M., Sasting M. and Pokharkar V.B., (2007). "*Pharmaceautical research*" 24, 1415.

Catena G.C. and Bright F. V. (1989). "*Thermodynamic study of the effects of B-Cyclodextrin Inclusion with Anilinonaphthalenesulphonates*". Analytical Chemistry, Vol. **61**, 905-906.

Chamberain J., Gibbs,J.E. and Gebbie H.E. (1969). "*The determination of refractive index spectra by fourier spectrometry*". Infrared Physics, Vol.**9**, no. 4, 189–209.

Chang B. and Park S. (2010). "*Electrochemical Impedance Spectroscopy*". Annual Review of Analytical Chemistry, Vol. **3**, 208-209.

Chaubey A. and Malhotra B.D. (2002). "*Mediated Biosensors*". Biosensors and Bioelectronics, Vol. **17**, 441-446.

Chen Bing, Weimin Cai, Jinheng Li and Xiaomei Ca, (2009). "Estimating N-acetyltransferase metabolic activity and pharmacokinetic Parameters of Isoniazid from genotypes in Chinese subjects". Clinica Chimica Acta, Vol. **405**, 23-29.

Clayton B. D. and Stock Y. N. (2001). "*Basic Pharmacology for Nurses*". Twelfth Edition, Mosby Inc: Missouri, 574-576.

Conn E.E., Stumff P.K. and Brueninig G. (1987). "*Outline of Biochemistry*". Fifth Edition, John Wiley and Sons, 115-163.

Craig C. R. and Stitzel R. E. (1990). "*Modern Pharmacology*". Third Edition, Little, Brown and Company: Boston, 700-708.

Cresphilho F., Travains S. A. and Oliveira Jr. O.N. (2009). "*Enzyme immobilization on Ag nanoparticles/polyaniline nanocomposite*". Biosensors and Bioelectronics, Vol. **24**, 3073-3074.

Cullity B. D. (1978). *"Elements of X-ray diffraction"*. 2nd ed. Addison-Wesley, Reading, Mass.

D'Orazio P. (2003). "Biosensors in clinical chemistry". Clinica Chimica Acta, Vol. **334**, 41-42.

De Groot M. J. and Ekins S. (2002). *"Pharmacophore modelling of cytochrome P450"*. Advanced Drug Delivery Reviews, Vol. **54**, 375-376.

Donat Ivan, Andrea Travan, Chiara Pelillo, Tommaso Scarpa, Anna Coslov, Alois Bonfacio, Valter Sergo and Sergio paoletti, (2009). "Polyol synthesis of silver nanoparticles: Mechanism of reduction by Alditol Bearing Polysaccharides". Biomacromolecules, Vol. **10**, no.2, 210-213.

Eoh H. and Brennan P.J. (2009). *"The Mycobacterium tuberculosis MEP (2C-methyl-D-erythritol 4-phosphate) pathway as a new drug target"*. Tuberculosis, Vol. **89**, 1-2.

Evanoff Jr. D.D. and Chumanov G. (2004). *"Size-controlled synthesis of nanoparticles"*. "Silver-only" aqueous suspensions via hydrogen reduction. J. Phys. Chem. B., Vol.**108**, 13948–13956.

Fernandes J.B. and Kubota L.T. (1999). *"Potentiometric biosensor for L-ascorbic acid based on ascorbate oxidase of natural source immobilzed on ethylene-vinlacetate membrane"*. Analytica Chima Acta, Vol. **385**, 3-1.

Gerard M. and Chaubey A. (2002). "Application of conducting polymers to biosensor". Biosensors and Bioelectronics, Vol. **17**, 346-347.

He R., Chian X., Yin J., Zhu Z and Mater J. (2002). Chem. Vol. **12**, 3783.

Hagedoorn P. L., de Geus D.C. and Hagen W.R. (2002). *"Spectroscopic characterization and ligand-binding properties of chlorite dismutase from the chlorate respiring bacterial strain GR-1"*. Europeun Journal of Biochemistry, Vol. **269**, 4906-4907.

Harris D., Loew G. and Waskell L. (2001). *"Calculation of the electronic structure and spectra of model cytochrome P450 compound I"*. Journal of Inorganic Biochemistry, Vol. **83**, 309-311.

Hernandez C. and Cetner A., (2008). "Tuberculosis in the age of biologic therapy". Journal of American Academy of Dermatology, Vol. **59**, No 3, 363-364.

Hertog M.G.L, Hollman P.C.H and Van de putte B, (1993). Agric. Food Chem. Vol. **41**, 1242.

Hou Y. *et al.*, (2005). Applied Surface Science, Vol. **241**, 218- 222.

Hu J, L,-S. Li, and A.P. Alivistos, (2001). ''Band gap variation of siz e and shape controlled colloidal Cdse quantum rods'' Nano Letters, Vol. **1**, no. 7, 349-35.

Huang L., Liao W., Ling H. and Wen T., (2009). *"Simultaneous synthesis of polyaniline nanofibers and metal (Ag and Pt) nanoparticles"*. Materials Chemistry and Physics, Vol. **116**, 474-475.

Hutchison J.E., (2008). *"Greener nanoscience: a proactive approach to advancing applications and reducing implications of nanotechnology"*. ACS nano, vol. **2**, no.3, 395-402.

Iwuoha E.I., and Smyth M.R., (2003). *"Reactivities of organic phase: 6.Square-wave and differential pulse studies of genetically engineered cytochrome $P450_{cam}$ (CYP101) bioelectrodes in selected solvents"*. Biosensors and Bioelectronics, Vol. **18**, 237-238.

Jenkel J., (1994). *"Analytical Chemistry for Technicians"*. Lewis Publishers, Boca Raton, United States of America.

Jiang Z.-J, C.-Y and Sun L.-W, (2004). Catalytic properties of silver nanoparticles supported on silica spheres.

Joseph S. and Rusling J. F., (2003). "An amperometric biosensor with human CYP3A4 as a novel drug screening tool" Biochemical Pharmacology, Vol. **65,** 1817-1818.

Key E.R.M., (1966). Biochemistry Collier-Macmillan Limited, London, 290-291.

Kumar C. G. and Mamidyala S. K., (2011). *"Extracellular synthesis of silver nanoparticles using culture supernatant of Pseudomonus aeruginosa"*. Colloids and Surfaces B: Biointerfaces, Vol. **84,** 463-464.

Lesney M. S., (2002). *"Today's Chemistry at Work"*. American Chemical Society, Vol. **1,** 33-34.

Li M., Gao Y., Wang G. and Fang B., (2005). *"Preparation of novel mercury-doped silver nanoparticles film glassy carbon electrode and its application for electrochemical biosensor"*. Analytical Biochemistry, Vol. **341,** 52-53.

Lindfors T. and Ivaska A., (2002). "Potentiometric and UV-vis characterisation of N-substituted polyanilines". Journal of Electroanalytical Chemistry, Vol. **535,** 69-71.

Liu C. and Hu J., (2009). *"Hydrogen peroxide biosensor based on the direct electrochemistry of myoglobin immobilized on silver nanoparticles doped carbon nanotubes film"*. Biosensors and Bioelectronics, Vol. **24,** 2149-2150.

Malhotra B.D. and Chaubey A., (2006). *"Prospects of conducting polymers in biosensors"* Analytica Chimica Acta, Vol. **578,** 60-61.

Mallikarjuns K., John N. Sushma, Narasimha G., Venkateswara K. Rao, Manoj L. and Deva B., (2011). *"Prasad Raju in International Conference on Nanoscience Engineering and Technology"* ICONSET.

Mathebe Ntlatseng G.R., Aoife Morrin and Emmanuel I. Iwuoha, (2004). *"Electrochemitry and scanning electron microscopy of polyaniline/peroxide-based biosensor"*. Talanta, Vol. 64. 115-120.

Meyers F. H., Jawetz E. and Goldfien A., (1980). *"Review of Medical Pharmacology"*. Seventh Edition, Lange Medical Publication Ltd: California, 565-567.

Moltke Von L.L., Greenbalt D.J., Duan S.X. and Shader R.I., (1997). *"Human cytochromes mediating N-demethylation of fluoxetine in vitro"*. Psychopharmacology, Vol. 132, 402-407.

Moore D. M. and R. C. Reynolds Jr., (1997). *"X-Ray diffraction and the identification and analysis of clay minerals"*. 2nd Ed. Oxford University Press, New York.

Mu S., Cheng C. and Wang J., (1997). *"The kinetic behaviour for the electrochemical polymerization of aniline in aqueous solution"*. Synthetic Metals, Vol. 88, 249-254.

Mu S., Qu Y. and Jiang L., (2009). *"Effect of refluxed silver nanoparticles on inhibition and enhancement of enzymatic activity of glucose oxidase"*. Colloids and Surfaces A: Physiochemical Engineering Aspects, Vol. 345, 101-102.

Muchindu Mukombwe, Tesfaye Waryo, Omatayo Arotiba, Ewakarzimierska, Aoif Morrin, Anthony J. Killard, Malcom R. Smyth, Nazeem Jahed, Boitumelo Kgarebe, Priscilla G.L. Baker, Emmanuel I. Iwuoha, (2010). *"Electrochemical nitrate nanosensor developed with amine and sulphate functonalised polystyrene latex beads self assembled on polyaniline"*. Electrochemical Acta, Vol. 55, 4274- 4280.

Nadagouda M. N., Castle A.B., Murdock R.C., Hussain S.M. and Varma R.S., (2010). *"In vitrobiocompatibility of nanoscale zerovalent iron particles (NZVI) synthesized using tea polyphenols"*. Green Chem. Vol. 12, 114–122.

Nadagouda M. N. and Rajender S. Varma, (2008). *"Green synthesis of silver and palladium nanoparticles at room temperature using coffee and tea extract"*. Green Chem.Vol. **10**. 859-862.

Naznin Ara Begum, Samira Mondal, Sawat Basu, Rajibu A. Laskar and Debarabrata Mandal, (2009). *"Biogenic synthesis of of Au and Ag nanoparticles using aqueous solutions of black Tea leaf extracts"*. Colloids and Surfaces B: Biointerfaces, Vol. **71**, 113- 118.

Naudin E., Gouerec P. and Belanger D., (1998). *"Electrochemical preparation and characterization in non-aqueous electrolyte of polyaniline electrochemically prepared from an anilinium salt"*. Journal of Electroanalytical Chemistry, Vol. **1**, 459.

Nyholm Leif, (2005). *"Electrochemical techniques for a lab-on-a-chip application"*. Analyst, Vol. **130**. 4274-4280.

Paddle B. M., (1996). *"Biosensors for chemical and biological agents of defense interest"*. Biosensors and Bioelectronics, Vol. **11**, 1079-1083.

Pandey P.C. and Prakash R., (1998). *"Polyindole modified potassium ion-sensor using dibenzo-18-crown-6 mediated PVC matrix membrane"*. Sensors and Actuators B, Vol. **46**, 61-62.

Patrick G. L., (2005). "Medical Chemistry". Third Edition, Oxford University Press Ltd: New York, 381-282.

Porubsky P.R. and Meneely K. M., (2008). *"Structures of Human Cytochrome P-450-2E1"*. Journal of Biological Chemistry, Vol. **48**, 33698-33701.

Russell S. D. and Daghlian, C. P., (1985). *"Scanning electron microscopic observations on deembedded biological tissue sections: Comparison of different fixatives and embedding materials"*.

Ryne-Byrne S., (1997). *"Development of and Amperometric anti-biotin Immunosesnor"*. Thesis, Dublin City University.

Sadik O.A., Mwilu S. K. and Aluoch A., (2009). *"Smart Electrochemical Biosensors: From advanced materials to ultrasensitive devices"*. Ewlectrochimica Acta, Vol. **55**, 4290-4291.

Sarkar P. and Bhui D. K., (2009). *"Synthesis and photophysical study of silver nanoparticles stabilized by unsaturated dicarboxylates"*. Journal of Luminescence, Vol. **129**, 704-705.

Sathishkumar M., Won S.W., Cho C-W. and Yun Y-S., (2009). *"Cinnamon zeyanicum bark extract and powder mediated green synthesis of nano-crystalline silver particles and its bactericidal activity"*. Colloids and Surfaces B: Biointerfaces, Vol. **73**, 336-337.

Schweon S.J., (2009). *"Tuberculosis Update"*. Journal of Radiology and Nursing, Vol. **28** 12-14.

Sharma V.K, Ria A.Yngard and Yaketerina Lin, (2009). "Silver nanoparticles: Green synthesis and their antimicrobial activities". Advances in colloid and Interface science, Vol. **145**, 83-96.

Shumyantseva V.V., Bulko T.V. and Archakov A.I., (2007). *"Electrochemical properties of cytochroms P450 using nanostructured electrodes: Direct electron transfer and electro catalysis"* Journal of Inorganic Biochemistry, Vol. **101**, 859-860.

Shumyantseva V.V., Bulko T.V. and Archakov A.I., (2005). "Electrochemical reduction of Cytochrome P450 as an approach to the construction of biosensors and bioreactors". Journal of Inorganic Biochemistry, Vol. **99**, 1057-1058.

Siddiqui S., Chen H., Li J. and Meyyappan M., (2010). *"Characterization of Carbon Nanofiber Electrode Arrays Using Electrochemical Impedance Spectroscopy: effect of Scaling down Electrode Size"*. American Chemical Society, Vol. **4**, 955-956.

Skoog D. A., West D. M. and Holler F. J., (1992). *"Fundamentals of Analytical Chemistry"*. Saunders College Publishing, Fort Worth, United States of America, 100-200.

Songa E.A., Arotiba O.A., Jahed N., (2009). *"Electrochemical detection of glyphosate herbicide using horseradish peroxidise immobilized of sulfonated polymer matrix"*. Bioelectrochemistry, Vol. 75, 121-122.

Spracklin D.K. and Hankins D. C., (1997). *"Cytochrome P450 2E1 is the Principal Catalyst of Human Oxidative Halothane Metabolism in Vitro"*. The Journal of Pharmacololgy and Experimental Therapeutics, Vol. 1, 401-402.

Sun X., He P., Liu P. and Fang Y., (1998). *"Immobilization of single-stranded deoxyribonucleic acid on gold electrode with self-assembled aminoethanethiol monolayer for DNA electrochemical sensor applications"*. Talanta, Vol. 47, 487-488.

Tran-Van F., Henri T. and Cverot C., (2002). *"Synthesis and electrochemical properties of mixed ionic and electronic modified polycarbazole"*. Electrochimica acta, Vol. 47, 2927-2928.

Trivedi D. C., (1996). "Handbook of Organic Conductive Molecules and Polymers: Volume 2 Conductive Polymers: Synthesis and Electrical Properties" John Wiley and Sons Ltd: New York. 506–572.

Wallis R.S. and Doherty T. M., (2009). *"Biomarkers for tuberculosis disease activity, cure and relapse"*. Lancet Infectious Disease, Vol. 9, 162-163.

Wang J., (2006). *"Electrochemical biosensors: Towards point-of-care cancer diagnostics"*. Biosensors and Bioelectronics, Vol. 21, 1889-1891.

Wang W. and Chen J., (2009). *"Tuberculosis of the head and neck: a review of 20 cases"*. Oral Surgery, Oral Medicine, Oral Pathology, Oral Radiology, and Endodotology, Vol. 107, 381-382.

Worsfold P.J., (1995). "Classification of immobilized enzymes". Pure and Applied Chemistry, Vol. 67, 597-600.

Xia Lin, Zhixiang Wei, and Meixiang Wan, (2010). "*Conducting polymer nanostructures and their application in nanobiosensors*". Journal of colloid and Interface Science. Vol. 341, 1-11.

Yoo J., Song I. and Park S., (2003). "*Real-Time Impedance Measurements during Electrochemical Experiments and Their Application to Aniline Oxidation*". Analytical Chemistry, Vol. 75, 3294-3295.

Zhang H.W. and Liu Y. (2010). "*Sun Front*". Phys, 5, 347.

Zhu N. and Chang Z., (2006). "*Electrochemically fabricated polyaniline nanowire-modified electrode for voltammetric detection of DNA hybridization*". Electrochimica Acta. Vol. 51, 3759-3760.

Zvavamwe Z. and Ehlers V., (2009). "*Experiences of a community-based tuberculosis treatment programme in Namibia: A comparative cohort study*". International Journal of nursing Studies, Vol. 46, 303-304.

APPENDIX

A. Calculation of percent yield of AgNPs corresponding to 25 °C.

A tomic mass of Ag, g.	-	107.8682 g
Number of Ag atoms Present in $AgNO_3$.	-	1
Mass percent of Ag in $AgNO_3$.	$\dfrac{107.8682}{169.9 \text{ (Mass of AgNO}_3)} \times 100$	63.449%
Mass of Ag^+ in 0.169 g of $AgNO_3$ (1mM) dissolved 1000 ml distilled water (stock solution), g.	$\dfrac{63.449}{100} \times 0.169$	0.10722881 g
Mass of Ag$^+$ in 5 ml aqueous solution of the 1000 ml aqueous solution, g.	$\dfrac{5 * 0.10722881}{1000}$	0.0005 g
Mass of tea-AgNPs synthesized (Weighed), g.	-	0.0001 g
Percent yield	$\dfrac{0.0001}{0.0005} \times 100$	20 %

-89-

B. Calculation of percent yield of AgNPs corresponding to 30 °C.

A tomic mass of Ag, g.	-	107.8682 g
Number of Ag atoms Present in AgNO$_3$.	-	1
Mass percent of Ag in AgNO$_3$.	$\dfrac{107.8682}{169.9 \,(\text{Mass of AgNO}_3)} \times 100$	63.449%
Mass of Ag$^+$ in 0.169 g of AgNO$_3$ (1mM) dissolved 1000 ml distilled water (stock solution), g.	$\dfrac{63.449}{100} \times 0.169$	0.10722881 g
Mass of Ag$^+$ in 5 ml aqueous solution of the 1000 ml aqueous solution, g.	$\dfrac{5* 0.10722881}{1000}$	0.0005 g
Mass of tea-AgNPs synthesized (Weighed), g.	-	0.0002 g
Percent yield	$\dfrac{0.0002}{0.0005} \times 100$	40 %

C. Calculation of percent yield of AgNPs corresponding to 50 °C.

Atomic mass of Ag, g.	-	107.8682 g
Number of Ag atoms Present in $AgNO_3$.	-	1
Mass percent of Ag in $AgNO_3$,	$\dfrac{107.8682}{169.9 \text{ (Mass of AgNO}_3)} \times 100$	63.449%
Mass of Ag^+ in 0.169 g of $AgNO_3$ (1mM) dissolved 1000 ml distilled water (stock solution), g.	$\dfrac{63.449}{100} \times 0.169$	0.10722881 g
Mass of Ag^+ in 5 ml aqueous solution of the 1000 ml aqueous solution, g.	$\dfrac{5 * 0.10722881}{1000}$	0.0005 g
Mass of tea-AgNPs synthesized (Weighed), g.	-	0.0002 g
Percent yield	$\dfrac{0.0002}{0.0005} \times 100$	40 %

D. **Calculation of percent yield of AgNPs corresponding to 70 °C.**

A tomic mass of Ag, g.	-	107.8682 g
Number of Ag atoms Present in AgNO$_3$.	-	1
Mass percent of Ag in AgNO$_3$.	$\dfrac{107.8682}{169.9 \,(\text{Mass of AgNO}_3)} \times 100$	63.449%
Mass of Ag$^+$ in 0.169 g of AgNO$_3$ (1mM) dissolved 1000 ml distilled water (stock solution), g.	$\dfrac{63.449}{100} \times 0.169$	0.10722881 g
Mass of Ag$^+$ in 5 ml aqueous solution of the 1000 ml aqueous solution, g.	$\dfrac{5 * 0.10722881}{1000}$	0.0005 g
Mass of tea-AgNPs synthesized (Weighed), g.	-	0.0003 g
Percent yield	$\dfrac{0.0003}{0.0005} \times 100$	60 %